Electroweak Theory in the Standard Model

From Fermi Theory to Flavour and Grand Unification

Dr Bipasha Chakraborty
School of Physics and Astronomy, University of Southampton

STFC HEP Summer School

September 2026

Contents

Preface **iv**

1 From Fermi Theory to Electroweak Gauge Theory **1**

1.1 The Standard Model and quantum field theory . . . 1

1.1.1 A brief reminder: QED . . . 2

1.1.2 A brief reminder: QCD . . . 2

1.2 What is a gauge group? A minimal introduction . . . 3

1.3 Experimental clues from weak interactions . . . 3

1.4 Chirality and the $V - A$ current . . . 4

1.5 Fermi's four-fermion theory . . . 5

1.6 The W boson resolves the contact interaction . . . 6

1.7 Why adding a massive vector boson is not enough . . . 7

1.8 From chiral currents to $SU(2)_L$ doublets . . . 7

1.9 Summary and outlook . . . 8

2 Building the Electroweak Gauge Theory **9**

2.1 The observations that the theory must explain . . . 9

2.2 The minimum group theory needed . . . 10

2.2.1 Doublets, singlets and generators . . . 10

2.2.2 The $U(1)_Y$ factor . . . 10

2.3 The fermions and their electroweak charges . . . 11

2.4 Local symmetry and the covariant derivative . . . 11

2.5 The charged-current interaction . . . 12

2.6 Neutral currents: the photon and Z . . . 13

2.7 What gauge symmetry predicts—and the remaining problem . . . 14

2.8 Summary . . . 14

3 Electroweak Symmetry Breaking **16**

3.1 What does spontaneous symmetry breaking mean? . . . 16

3.2 The electroweak scalar sector . . . 17

3.3 Deriving the gauge-boson masses . . . 18
3.3.1 The charged sector . . . 18
3.3.2 The neutral sector . . . 19
3.4 The electroweak scale from muon decay . . . 19
3.5 The physical Higgs boson . . . 20
3.6 Fermion masses and the remaining flavour puzzle . . . 21
3.7 What the mechanism predicts . . . 22
3.8 Putting the pieces together: the electroweak Lagrangian . . . 22
3.9 Summary . . . 23

4 Electroweak Phenomenology **25**
4.1 The electroweak interactions in the mass basis . . . 25
4.2 From the electroweak Lagrangian to Feynman diagrams . . . 26
4.2.1 From an interaction term to a vertex . . . 26
4.2.2 External particles and internal lines . . . 27
4.2.3 Electroweak fermion vertices . . . 27
4.2.4 Worked example: leptonic W decay . . . 28
4.2.5 Spin and polarisation sums . . . 28
4.2.6 Z-boson decay . . . 29
4.2.7 Scattering example: $e^+e^- \to f\bar{f}$ . . . 29
4.2.8 From a scattering amplitude to a cross section . . . 30
4.3 Decay widths: turning vertices into observables . . . 31
4.3.1 Why weak widths contain $G_F M^3$ . . . 31
4.3.2 Leptonic W decay . . . 32
4.3.3 Z partial widths . . . 33
4.4 Resonances and the Z line shape . . . 34
4.5 Angular distributions and parity-violating asymmetries . . . 34
4.6 Charged-current production and the special problem of m_W . . . 35
4.7 Low-energy neutral-current checks . . . 35
4.8 Choosing electroweak input parameters . . . 36
4.9 Radiative corrections: sensitivity to virtual heavy particles . . . 36
4.10 Interpreting a deviation . . . 37
4.11 Summary . . . 37

5 Flavour Physics and Muon $g-2$ **39**
The three generations of quarks and leptons . . . 39
5.1 Flavour begins with the Yukawa matrices . . . 40

5.2 Why is it called the CKM matrix? . . . 41
5.3 The structure and parameters of the CKM matrix . . . 41
5.4 Unitarity triangles . . . 42
5.4.1 Constructing the unitarity triangle . . . 42
5.4.2 How CKM unitarity provides precision tests . . . 43
5.5 How CP violation appears . . . 46
5.6 The GIM mechanism and rare neutral currents . . . 48
5.7 Current experimental flavour connections . . . 49
5.8 Magnetic moments and the meaning of $g-2$ . . . 49
5.9 How a_μ is measured . . . 50
5.10 The Standard Model prediction for a_μ . . . 51
5.10.1 QED: photon and charged-lepton loops . . . 51
5.10.2 Electroweak loops . . . 51
5.10.3 Hadronic vacuum polarisation . . . 52
5.10.4 Hadronic light-by-light scattering . . . 52
5.10.5 Precision accounting . . . 52
5.10.6 Present comparison with experiment . . . 53
5.11 Summary . . . 53

6 Grand Unification **55**
6.1 A minimal group-theory dictionary . . . 55
6.2 Running couplings: why unification can be hidden . . . 56
6.3 $SU(5)$: the minimal worked example . . . 56
6.4 Proton decay: the decisive consequence . . . 58
6.5 $SO(10)$, neutrino mass and the seesaw . . . 58
6.6 What can low-energy experiments really test? . . . 59
6.7 Summary . . . 59

Preface

These notes accompany six lectures for experimental particle-physics PhD students at the STFC HEP Summer School. They assume a working knowledge of quantum mechanics, special relativity and the basic methods of quantum field theory, but no prior knowledge of group theory. The emphasis is on the physical logic connecting experimental observations to the electroweak Standard Model, its flavour structure, precision tests and possible grand unification. These lectures are based on my previous three separate lectures and inspired by PhD course lectures at the University of Glasgow and the University of Kentucky. I acknowledge the use of ChatGPT for rearranging and restructuring.

QED, QCD and the general machinery of quantum field theory are assumed to have been taught separately. The course therefore concentrates on the electroweak sector. Group theory is introduced only when it is needed to interpret a field or interaction. Each lecture follows the same pattern: physical motivation, one central derivation, an experimental connection and a short summary.

Six-lecture structure

Lecture 1: Fermi theory to gauge theory. The experimental features of weak interactions, chirality and $V-A$, the Fermi interaction, W exchange, and why a gauge-theory completion is required.

Lecture 2: Electroweak gauge structure. The minimum group theory needed for $SU(2)_L \times U(1)_Y$, fermion doublets and singlets, hypercharge, charged currents, and photon–Z mixing.

Lecture 3: Electroweak symmetry breaking. The Higgs potential and vacuum, derivation of m_W, m_Z and the massless photon, the scale $v \simeq 246$ GeV, and Higgs couplings to matter.

Lecture 4: Electroweak phenomenology. W and Z decay widths, the Z line shape, angular asymmetries, experimental determination of m_W, electroweak input parameters and radiative corrections.

Lecture 5: Flavour and the muon magnetic moment. The Yukawa origin of CKM mixing, unitarity triangles, CP violation, GIM suppression, selected flavour measurements, and the present interpretation of muon $g-2$.

Lecture 6: Grand unification. Running gauge couplings, the minimal $SU(5)$ example, proton decay, $SO(10)$ and the seesaw, and how low-energy experiments test very high scales.

Chapter 1

From Fermi Theory to Electroweak Gauge Theory

The Standard Model is a relativistic quantum field theory of the known elementary particles and their strong, electromagnetic and weak interactions. This lecture first places the Standard Model within quantum field theory and briefly recalls the gauge-theory structures of QED and QCD. We then build the motivation for the electroweak theory from observed properties of weak processes. Fermi's four-fermion description is introduced as an effective low-energy theory, and its relation to the exchange of a massive charged vector boson is derived. The chiral structure of the weak current naturally leads to left-handed fermion doublets and, ultimately, to an $SU(2)_L \times U(1)_Y$ gauge theory. No previous knowledge of group theory is assumed.

1.1 The Standard Model and quantum field theory

The Standard Model (SM) is our most precise description of elementary-particle physics. It identifies a small set of fields—quarks, leptons, gauge fields and the Higgs field—and specifies how these fields interact. Its predictions range from particle lifetimes and scattering cross sections to the magnetic moments of leptons and the properties of the W, Z and Higgs bosons. In a large variety of experiments, these predictions agree with observation to remarkable accuracy.

The Standard Model is not merely a list of particles. It is a particular *quantum field theory* (QFT). In QFT, particles are excitations of fields: an electron is an excitation of an electron field, a photon is an excitation of the electromagnetic field, and so on. Relativistic causality, quantum mechanics and symmetry severely restrict the interactions that these fields can have. The dynamics are encoded in a Lagrangian density,

$$\mathcal{L} = \mathcal{L}_{\text{kinetic}} + \mathcal{L}_{\text{interaction}}, \tag{1.1}$$

and observable amplitudes are calculated perturbatively using propagators and interaction vertices, or non-perturbatively when the coupling is strong.

The gauge symmetry of the Standard Model is conventionally written

$$G_{\text{SM}} = SU(3)_C \times SU(2)_L \times U(1)_Y. \tag{1.2}$$

At first sight, this compact expression can seem to hide rather than explain the physics. Its meaning will be developed gradually. For now, the three factors encode three kinds of gauge interaction:

Gauge factor	Interaction	Gauge fields before symmetry breaking
$SU(3)_C$	strong	eight gluon fields G^a_μ
$SU(2)_L$	weak isospin	three fields $W^1_\mu, W^2_\mu, W^3_\mu$
$U(1)_Y$	weak hypercharge	one field B_μ

The photon and the physical Z boson are not initially present as separate gauge fields: they emerge as different mixtures of W^3_μ and B_μ after electroweak symmetry breaking. Understanding why this happens will be the central task of Lectures 2 and 3.

1.1.1 A brief reminder: QED

Quantum electrodynamics (QED) describes charged fermions interacting with the electromagnetic field. For one Dirac fermion of electric charge qe, its Lagrangian is

$$\mathcal{L}_{\text{QED}} = -\frac{1}{4}F_{\mu\nu}F^{\mu\nu} + \bar{\psi}(i\gamma^\mu D_\mu - m)\psi, \qquad D_\mu = \partial_\mu + ieqA_\mu, \tag{1.3}$$

where

$$F_{\mu\nu} = \partial_\mu A_\nu - \partial_\nu A_\mu. \tag{1.4}$$

The interaction term follows immediately by expanding the covariant derivative:

$$\mathcal{L}_{\text{int}} = -eq\,\bar{\psi}\gamma^\mu\psi A_\mu. \tag{1.5}$$

Thus the gauge principle fixes the Lorentz structure of the interaction. It does not merely state that electric charge is conserved; it specifies how the photon couples to the conserved current.

QED is based on the group $U(1)$. Operationally, $U(1)$ means that a field may be multiplied by a phase,

$$\psi(x) \longrightarrow e^{iq\alpha(x)}\psi(x), \tag{1.6}$$

without changing physical predictions. When the phase is allowed to depend on space-time, the ordinary derivative of the transformed field contains an unwanted term proportional to $\partial_\mu\alpha$. Introducing A_μ and replacing ∂_μ by D_μ restores covariance. The photon is therefore not added arbitrarily: it is required by local phase invariance.

1.1.2 A brief reminder: QCD

Quantum chromodynamics (QCD) applies the gauge principle to colour. A quark field has three colour components,

$$q(x) = \begin{pmatrix} q_r(x) \\ q_g(x) \\ q_b(x) \end{pmatrix}, \tag{1.7}$$

which can be mixed by local $SU(3)_C$ transformations. The covariant derivative is

$$D_\mu = \partial_\mu + ig_s T^a G^a_\mu, \tag{1.8}$$

where the index $a = 1, \ldots, 8$ labels the eight gluon fields. Unlike the photon, gluons themselves carry the relevant gauge charge. Consequently, the QCD field strength contains nonlinear terms,

$$G^a_{\mu\nu} = \partial_\mu G^a_\nu - \partial_\nu G^a_\mu + g_s f^{abc} G^b_\mu G^c_\nu, \tag{1.9}$$

which generate three- and four-gluon interactions. These self-interactions are essential to asymptotic freedom and confinement.

For the present course, the important lesson from QED and QCD is structural:

Key idea

A local gauge symmetry determines the gauge fields, their couplings to matter and, in a non-Abelian theory, their self-interactions. Electroweak theory uses the same principle, but its action on left- and right-handed fermions is different. It is therefore a *chiral* gauge theory.

1.2 What is a gauge group? A minimal introduction

A group is a set of transformations that can be composed and inverted and that includes an identity transformation. In particle physics, the transformations often change the internal description of a field without changing observable physics. The word *internal* means that the transformations act on field components rather than directly on space-time coordinates.

Continuous groups contain transformations arbitrarily close to the identity. Near the identity, a transformation can be written as

$$U(\boldsymbol{\alpha}) = \exp(i\alpha^a T^a) \simeq 1 + i\alpha^a T^a + \cdots . \tag{1.10}$$

The matrices T^a are called *generators*. They specify how the transformation acts on the field. The number of independent generators equals the number of gauge fields required when the symmetry is made local.

The word *representation* simply describes which matrices act on a particular field. A field that is unchanged by a group transformation is called a singlet. Two field components that transform into linear combinations of one another form a doublet. No abstract representation theory is needed for our first encounter with electroweak physics.

For $U(1)$ there is one continuous parameter and hence one generator and one gauge field. The generator acting on a given field is its $U(1)$ charge. For $SU(2)$ in its two-component representation, we may choose

$$T^a = \frac{\sigma^a}{2}, \tag{1.11}$$

where σ^a are the Pauli matrices. There are three generators, and therefore three gauge fields. The familiar Pauli matrices make $SU(2)$ a natural language whenever two states are mixed, but in electroweak theory the two components represent different particles rather than spin-up and spin-down states.

Checkpoint

The notation $SU(2)_L$ does not mean that every fermion comes in a two-component multiplet. It means that the symmetry acts non-trivially on specified *left-handed* fermion doublets. The corresponding right-handed fields are $SU(2)_L$ singlets.

1.3 Experimental clues from weak interactions

Before constructing the electroweak theory, we should identify what it must explain. Weak interactions were first recognised in nuclear beta decay and later in muon and hadron decays.

Representative processes include

$$n \longrightarrow p + e^- + \bar{\nu}_e, \tag{1.12}$$
$$\mu^- \longrightarrow e^- + \bar{\nu}_e + \nu_\mu, \tag{1.13}$$
$$\pi^- \longrightarrow \mu^- + \bar{\nu}_\mu. \tag{1.14}$$

At the quark level, neutron beta decay contains the transition

$$d \longrightarrow u + W^{-*}, \qquad W^{-*} \longrightarrow e^- + \bar{\nu}_e. \tag{1.15}$$

The asterisk indicates that the intermediate W is virtual.

The weak interaction differs sharply from electromagnetism. The photon is massless and couples to a flavour-diagonal vector current. The charged weak interaction is mediated by massive particles, changes flavour and distinguishes left from right. Weak neutral currents are also present, although they were discovered later because their experimental signature is less distinctive.

Property	Electromagnetic	Weak charged current	Weak neutral current
Mediator	γ	$W^\pm$	Z
Mediator mass	zero	nonzero	nonzero
Flavour change	no	yes	no at tree level
Chiral structure	same charge for L, R	left-handed fields only	different L, R couplings
Parity	conserved	violated	violated

Three clues will guide the construction:

1. charged-current weak interactions have a universal strength;
2. the charged current connects pairs such as (ν_e, e) and (u, d);
3. only left-handed fermion fields participate in the charged current.

1.4 Chirality and the $V - A$ current

For a Dirac field, define the chiral projection operators

$$P_L = \frac{1-\gamma^5}{2}, \qquad P_R = \frac{1+\gamma^5}{2}. \tag{1.16}$$

They satisfy

$$P_L^2 = P_L, qquad P_R^2 = P_R, qquad P_L P_R = 0, qquad P_L + P_R = 1. \tag{1.17}$$

The left- and right-handed parts of a field are

$$\psi_L = P_L \psi, \qquad \psi_R = P_R \psi, \qquad \psi = \psi_L + \psi_R. \tag{1.18}$$

The charged weak current has the vector-minus-axial-vector structure

$$J^\mu = \bar{\psi}_1 \gamma^\mu (1-\gamma^5) \psi_2 = 2\bar{\psi}_1 \gamma^\mu P_L \psi_2. \tag{1.19}$$

Thus it acts only on the left-handed component of the second fermion field. This is the field-theoretic expression of maximal parity violation in charged-current processes.

For example, the leptonic charged current is

$$J_+^\mu = \bar{\nu}_{eL}\gamma^\mu e_L + \bar{\nu}_{\mu L}\gamma^\mu \mu_L + \bar{\nu}_{\tau L}\gamma^\mu \tau_L, \tag{1.20}$$

with $J_-^\mu = (J_+^\mu)^\dagger$. In a later lecture, the quark current will acquire the Cabibbo–Kobayashi–Maskawa matrix because the weak-interaction and mass eigenstates of the quarks are not identical.

Experimental connection

The 1957 Wu experiment observed an angular asymmetry in the beta decay of polarised cobalt-60 nuclei. The result demonstrated that the weak interaction distinguishes a physical process from its mirror image. In modern language, the charged weak current contains left-handed fermion fields but not their right-handed partners.

For a massive particle, chirality and helicity are not identical. Helicity is the projection of spin along the direction of momentum and can change under a sufficiently fast Lorentz boost. Chirality is defined by γ^5 and is the quantity that appears directly in the electroweak Lagrangian. For an ultrarelativistic fermion, where $E \gg m$, chirality and helicity approximately coincide. This is why weak-interaction chirality is often described experimentally in terms of helicity.

1.5 Fermi's four-fermion theory

Fermi described beta decay through a local interaction among four fermion fields. In its modern $V - A$ form, the effective interaction for muon decay is

$$\mathcal{L}_F = -\frac{G_F}{\sqrt{2}}\left[\bar{\nu}_\mu \gamma^\alpha (1-\gamma^5)\mu\right]\left[\bar{e}\gamma_\alpha(1-\gamma^5)\nu_e\right] + \text{h.c.} \tag{1.21}$$

The four fermion fields meet at a single space-time point. At leading order, and neglecting the electron mass, the muon decay rate is

$$\Gamma(\mu^- \to e^-\bar{\nu}_e\nu_\mu) = \frac{G_F^2 m_\mu^5}{192\pi^3}\left(1 + \text{radiative and mass corrections}\right). \tag{1.22}$$

Consequently, the precisely measured muon lifetime determines G_F with very high precision. This same constant describes nuclear beta decay after the appropriate quark mixing and hadronic matrix elements are included. The common strength is a manifestation of weak universality.

Fermi theory is extremely successful at low energies, but its structure tells us that it cannot be fundamental. In four space-time dimensions a fermion field has mass dimension $3/2$. The operator in Eq. (1.21) therefore has dimension six:

$$[\bar{\psi}\psi\bar{\psi}\psi] = 6. \tag{1.23}$$

Since a Lagrangian density has dimension four,

$$[G_F] = -2. \tag{1.24}$$

The dimensionless expansion parameter at energy E is consequently of order

$$G_F E^2. \tag{1.25}$$

Amplitudes grow with energy, perturbation theory ultimately fails, and a point-like description cannot remain valid indefinitely. Equivalently, the theory is non-renormalisable: higher-order calculations require an increasing number of independent short-distance counterterms.

This does not make Fermi theory wrong. It makes it an *effective field theory*. It is the first term in a low-energy expansion in powers of E/M, where M is the mass scale of additional short-distance physics.

Key idea

Non-renormalisable does not mean useless or inconsistent within its domain of validity. Fermi theory is predictive when $E \ll M_W$. Its failure at high energy is valuable: it tells us that new propagating degrees of freedom must appear.

1.6 The W boson resolves the contact interaction

Suppose the charged current couples to a massive vector field according to

$$\mathcal{L}_{\mathrm{CC}} = -\frac{g}{2\sqrt{2}}\left(J_+^\mu W_\mu^+ + J_-^\mu W_\mu^-\right), \tag{1.26}$$

where our current J^μ contains the factor $(1-\gamma^5)$. The exchange of a W boson between two charged currents contains the propagator factor

$$\frac{-i}{q^2 - M_W^2}. \tag{1.27}$$

For momentum transfers much smaller than the W mass,

$$|q^2| \ll M_W^2, \tag{1.28}$$

we may expand

$$\frac{1}{q^2 - M_W^2} = -\frac{1}{M_W^2}\frac{1}{1 - q^2/M_W^2} \tag{1.29}$$

$$= -\frac{1}{M_W^2}\left(1 + \frac{q^2}{M_W^2} + \cdots\right). \tag{1.30}$$

Keeping only the leading term makes the propagator independent of momentum. In position space, the interaction therefore appears local. Combining the two vertices gives the effective coefficient

$$\boxed{\frac{G_F}{\sqrt{2}} = \frac{g^2}{8M_W^2}}. \tag{1.31}$$

Fermi theory is thus the low-energy limit of massive-W exchange. The corrections to the point-interaction approximation are suppressed by powers of q^2/M_W^2.

This matching relation already contains the electroweak scale. In Lecture 3 we will show that electroweak symmetry breaking gives

$$M_W = \frac{gv}{2}. \tag{1.32}$$

Substituting into Eq. (1.31) yields

$$v = (\sqrt{2}G_F)^{-1/2} \simeq 246 \text{ GeV}. \tag{1.33}$$

Thus a low-energy lifetime measurement determines the energy scale associated with the Higgs vacuum.

Experimental connection

Muon decay takes place at momentum transfers of order m_μ, far below M_W. The relative propagator correction is therefore roughly m_μ^2/M_W^2, explaining why the local Fermi interaction works extremely well. At collider energies comparable to or above M_W, the mediator is resolved and the full electroweak description is essential.

1.7 Why adding a massive vector boson is not enough

The intermediate-vector-boson picture improves the high-energy behaviour relative to a point interaction, but a massive spin-one field inserted by hand is not yet a complete electroweak theory. The longitudinal polarisation of a massive vector boson behaves increasingly strongly at high energy. Without the relations enforced by gauge symmetry, scattering amplitudes involving longitudinal W bosons grow too rapidly and violate perturbative unitarity.

Gauge symmetry supplies the necessary relations among fermion–gauge, triple-gauge and quartic-gauge interactions. However, an explicit mass term

$$\frac{1}{2}M_W^2 W_\mu W^\mu \tag{1.34}$$

is not invariant under the corresponding local gauge transformations. We therefore face an apparent conflict:

$$\text{gauge consistency suggests massless gauge fields,} \qquad \text{experiment finds massive } W^\pm \text{ and } Z. \tag{1.35}$$

The Higgs mechanism will resolve this conflict. The Lagrangian remains gauge invariant, but the vacuum is not invariant under the full electroweak symmetry. Three scalar degrees of freedom become the longitudinal polarisations of W^+, W^- and Z, while the photon remains massless.

1.8 From chiral currents to $SU(2)_L$ doublets

The charged weak current naturally groups left-handed fermions into pairs:

$$L_{eL} = \begin{pmatrix} \nu_{eL} \\ e_L \end{pmatrix}, \qquad L_{\mu L} = \begin{pmatrix} \nu_{\mu L} \\ \mu_L \end{pmatrix}, \qquad Q_L = \begin{pmatrix} u_L \\ d_L \end{pmatrix}. \tag{1.36}$$

The charged weak bosons move between the two components. In the fundamental two-component representation,

$$T^+ = \begin{pmatrix} 0 & 1 \\ 0 & 0 \end{pmatrix}, \qquad T^- = \begin{pmatrix} 0 & 0 \\ 1 & 0 \end{pmatrix}, \tag{1.37}$$

so that

$$T^+ \begin{pmatrix} 0 \\ 1 \end{pmatrix} = \begin{pmatrix} 1 \\ 0 \end{pmatrix}, \qquad T^- \begin{pmatrix} 1 \\ 0 \end{pmatrix} = \begin{pmatrix} 0 \\ 1 \end{pmatrix}. \tag{1.38}$$

This is the operational content of weak isospin raising and lowering. The right-handed charged fermions do not appear in such doublets because no right-handed charged current has been observed; they are $SU(2)_L$ singlets.

An $SU(2)_L$ theory alone cannot reproduce the observed electric charges. For example, the upper and lower members of a doublet differ in charge by one unit, but the average charge of the lepton doublet differs from that of the quark doublet. A further Abelian gauge factor, $U(1)_Y$, supplies the weak hypercharge Y. Electric charge will emerge as the combination

$$Q = T_3 + Y. \tag{1.39}$$

Lecture 2 will construct this theory explicitly, assign hypercharges to all fermion fields and show how the gauge fields couple to charged and neutral currents.

1.9 Summary and outlook

The main logical steps of this lecture are

$$\boxed{\begin{array}{c}\text{observed weak decays} \implies \text{local four-fermion interaction} \implies \text{massive } W \text{ exchange,}\\ \text{chirality and weak universality} \implies \text{left-handed doublets} \implies SU(2)_L \times U(1)_Y.\end{array}}$$

Fermi theory is a highly successful low-energy effective theory. Its dimension-six interaction and energy-growing amplitudes indicate that it cannot be fundamental. Massive-W exchange resolves the contact interaction and gives the matching relation $G_F/\sqrt{2} = g^2/(8M_W^2)$. The observed $V - A$ structure shows that weak interactions act differently on left- and right-handed fermions, motivating a chiral gauge theory. The unresolved question is how such a gauge theory can contain massive W and Z bosons while preserving a massless photon.

Checkpoint

Before Lecture 2, you should be able to answer:

1. In what sense is Fermi theory an effective field theory?
2. Why does the low-energy W propagator resemble a point interaction?
3. What does the subscript L in $SU(2)_L$ mean physically?
4. Why do three $SU(2)$ generators imply three gauge fields?
5. Why can $SU(2)_L$ alone not reproduce all observed electric charges?

Short exercises

1. Verify $P_L^2 = P_L$, $P_R^2 = P_R$ and $P_L P_R = 0$ using $(\gamma^5)^2 = 1$.
2. Expand the W propagator through order q^2/M_W^2 as in Eq. (1.30). Estimate m_μ^2/M_W^2 and comment on the accuracy of Fermi theory for muon decay.
3. Using dimensional analysis, show that a four-fermion operator has mass dimension six and that $G_F E^2$ is dimensionless.
4. Apply T^+ and T^- to both components of a two-component doublet. Which operations give zero, and why is that physically sensible?
5. The two members of the lepton doublet have charges $(0, -1)$, while those of the quark doublet have charges $(2/3, -1/3)$. Show that the charge difference within either doublet is one, but that their average charges differ. Why does this suggest an additional $U(1)$ quantum number?

Chapter 2

Building the Electroweak Gauge Theory

The purpose of the electroweak gauge group is not to add abstract mathematics to weak interactions. It is to encode, economically, which particles transform into one another and to relate many observed vertices to two gauge couplings.

Lecture 1 established three important facts. Weak charged currents have a $V - A$ form, they act on left-handed fermions, and at low energy they are described by Fermi's four-fermion interaction. We now build the theory that replaces the contact interaction by exchange of gauge bosons.

Only a small amount of group theory is needed. By the end of this lecture, we will be able to read the notation $SU(2)_L \times U(1)_Y$, understand why the weak interaction contains W^+, W^- and a neutral boson, derive the charged current, and show how the photon and Z arise from two neutral gauge fields.

2.1 The observations that the theory must explain

The charged weak interaction connects pairs of left-handed fermions:

$$\nu_{eL} \longleftrightarrow e_L, \qquad \nu_{\mu L} \longleftrightarrow \mu_L, \qquad u_L \longleftrightarrow d_L,$$

with analogous pairs in the other generations. A successful theory should explain why these transitions have a universal strength, why there are both charged and neutral weak currents, and why right-handed charged fermions do not participate in the charged current.

These observations suggest placing the two members of each pair into a two-component object, or *doublet*. Transformations that mix two complex components while preserving their norm form $SU(2)$. Because only left-handed fields participate, the relevant group is called $SU(2)_L$. The observed electric charges cannot be obtained from $SU(2)_L$ alone, so an additional Abelian factor $U(1)_Y$ is required. The electroweak gauge group is therefore

$$\boxed{G_{\mathrm{EW}} = SU(2)_L \times U(1)_Y.} \tag{2.1}$$

2.2 The minimum group theory needed

2.2.1 Doublets, singlets and generators

A symmetry transformation acts on a field multiplet. For example, a two-component field

$$\Psi = \begin{pmatrix} \psi_u \\ \psi_d \end{pmatrix}$$

may transform as $\Psi \to U\Psi$, where U is a 2×2 matrix. We call this a doublet representation. A field that is not mixed with another field is a singlet.

Continuous transformations close to the identity can be written as

$$U \simeq 1 + i\alpha^a T^a.$$

The matrices T^a are called generators. For the fundamental doublet of $SU(2)$, they are one half of the Pauli matrices:

$$T^1 = \frac{1}{2}\begin{pmatrix} 0 & 1 \\ 1 & 0 \end{pmatrix}, \qquad T^2 = \frac{1}{2}\begin{pmatrix} 0 & -i \\ i & 0 \end{pmatrix}, \qquad T^3 = \frac{1}{2}\begin{pmatrix} 1 & 0 \\ 0 & -1 \end{pmatrix}. \tag{2.2}$$

No general theory of Lie algebras is required here. We need only notice that T^3 is diagonal:

$$T_3\psi_u = +\frac{1}{2}\psi_u, \qquad T_3\psi_d = -\frac{1}{2}\psi_d.$$

The labels u and d simply mean upper and lower components; they need not denote quarks.

It is useful to combine the first two generators:

$$T^+ = T^1 + iT^2 = \begin{pmatrix} 0 & 1 \\ 0 & 0 \end{pmatrix}, \qquad T^- = T^1 - iT^2 = \begin{pmatrix} 0 & 0 \\ 1 & 0 \end{pmatrix}. \tag{2.3}$$

Acting with T^+ turns the lower component into the upper one, while T^- does the reverse:

$$T^+\begin{pmatrix} 0 \\ \psi_d \end{pmatrix} = \begin{pmatrix} \psi_d \\ 0 \end{pmatrix}, \qquad T^-\begin{pmatrix} \psi_u \\ 0 \end{pmatrix} = \begin{pmatrix} 0 \\ \psi_u \end{pmatrix}.$$

This is precisely the pattern required for charged weak transitions.

2.2.2 The $U(1)_Y$ factor

A $U(1)$ transformation multiplies a field by a phase,

$$\psi \longrightarrow e^{i\beta Y}\psi.$$

The number Y is weak hypercharge. It is not electric charge. Electric charge is the combination

$$\boxed{Q = T_3 + Y.} \tag{2.4}$$

For an $SU(2)_L$ singlet, all $SU(2)$ generators vanish, so $T_3 = 0$ and $Q = Y$.

Checkpoint

For this course, the essential group-theory dictionary is:

term	operational meaning
doublet	two fields mixed by $SU(2)_L$
singlet	$T^a = 0$
T_3	$+\frac{1}{2}$ for the upper entry, $-\frac{1}{2}$ for the lower
$T^{\pm}$	interchange the two entries
Y	the $U(1)_Y$ charge
Q	$T_3 + Y$

2.3 The fermions and their electroweak charges

For each generation, the left-handed fermions are weak doublets and the right-handed charged fermions are weak singlets:

$$Q_L = \begin{pmatrix} u_L \\ d_L \end{pmatrix} \sim (\mathbf{3}, \mathbf{2})_{1/6}, \qquad u_R \sim (\mathbf{3}, \mathbf{1})_{2/3}, \qquad d_R \sim (\mathbf{3}, \mathbf{1})_{-1/3}, \tag{2.5}$$

$$L_L = \begin{pmatrix} \nu_L \\ e_L \end{pmatrix} \sim (\mathbf{1}, \mathbf{2})_{-1/2}, \qquad e_R \sim (\mathbf{1}, \mathbf{1})_{-1}. \tag{2.6}$$

In $(\boldsymbol{d}_3, \boldsymbol{d}_2)_Y$, the first entry gives the dimension of the colour representation, the second gives the dimension of the weak representation, and the subscript is hypercharge. Thus **3** means a colour triplet, **2** a weak doublet and **1** a singlet.

Let us verify the charges rather than memorising the table. For the lepton doublet, $Y = -1/2$:

$$Q(\nu_L) = \frac{1}{2} - \frac{1}{2} = 0, \qquad Q(e_L) = -\frac{1}{2} - \frac{1}{2} = -1.$$

For the quark doublet, $Y = 1/6$:

$$Q(u_L) = \frac{1}{2} + \frac{1}{6} = \frac{2}{3}, \qquad Q(d_L) = -\frac{1}{2} + \frac{1}{6} = -\frac{1}{3}.$$

For the right-handed singlets, $T_3 = 0$, so their hypercharges are simply their electric charges.

The subscript L on $SU(2)_L$ is now concrete. An $SU(2)_L$ generator can turn ν_L into e_L, or u_L into d_L. For a right-handed singlet, $T^a f_R = 0$, so the charged-current interaction is absent. Parity violation is encoded in the field assignments rather than added later by hand.

Key idea

The Standard Model is a chiral gauge theory: left- and right-handed fermions are independent fields with different electroweak quantum numbers. They have the same electric charge after symmetry breaking, but they do not have the same weak interactions.

2.4 Local symmetry and the covariant derivative

If the transformation U is the same everywhere, the free kinetic term is invariant. If $U = U(x)$ varies with position, differentiating $U(x)\Psi(x)$ produces an unwanted term proportional to $\partial_\mu U$. Gauge fields are introduced so that this extra term is cancelled.

Operationally, the gauge principle tells us to replace

$$\partial_\mu \longrightarrow D_\mu = \partial_\mu + igT^a W_\mu^a + ig' Y B_\mu. \tag{2.7}$$

There are three $SU(2)_L$ generators, so there are three fields $W_\mu^1, W_\mu^2, W_\mu^3$, all with coupling g. The one generator of $U(1)_Y$ gives one field B_μ with coupling g'.

Expanding a fermion kinetic term gives

$$i\bar{\Psi}_L \gamma^\mu D_\mu \Psi_L = i\bar{\Psi}_L \gamma^\mu \partial_\mu \Psi_L - g\bar{\Psi}_L \gamma^\mu T^a \Psi_L W_\mu^a - g' Y \bar{\Psi}_L \gamma^\mu \Psi_L B_\mu. \tag{2.8}$$

The first term describes free propagation; the remaining terms are interactions. Once the representation and hypercharge are specified, their form is fixed. The same g applies to every weak doublet: this is weak universality.

2.5 The charged-current interaction

The fields W^1 and W^2 are more naturally written as charged combinations

$$W_\mu^\pm = \frac{W_\mu^1 \mp iW_\mu^2}{\sqrt{2}}. \tag{2.9}$$

Using

$$T^1 W_\mu^1 + T^2 W_\mu^2 = \frac{1}{\sqrt{2}} \left(T^+ W_\mu^+ + T^- W_\mu^- \right),$$

and $L_L = (\nu_L, e_L)^T$, the off-diagonal part of Eq. (2.8) becomes

$$\boxed{\mathcal{L}_{\rm cc}^\ell = -\frac{g}{\sqrt{2}} \left(\bar{\nu}_L \gamma^\mu e_L W_\mu^+ + \bar{e}_L \gamma^\mu \nu_L W_\mu^- \right).} \tag{2.10}$$

The two terms are Hermitian conjugates. Since $e_L = P_L e$,

$$\bar{\nu}_L \gamma^\mu e_L = \frac{1}{2} \bar{\nu} \gamma^\mu (1 - \gamma^5) e,$$

so the gauge-theory interaction reproduces the observed $V - A$ structure.

For quarks, the same calculation gives, for one generation,

$$\mathcal{L}_{\rm cc}^q = -\frac{g}{\sqrt{2}} \left(\bar{u}_L \gamma^\mu d_L W_\mu^+ + \bar{d}_L \gamma^\mu u_L W_\mu^- \right). \tag{2.11}$$

The extension to three generations introduces the CKM matrix and will be developed in Lecture 5.

Experimental connection

At a hadron collider, these vertices describe processes such as $u\bar{d} \to W^+ \to \ell^+ \nu$. The neutrino is inferred from missing transverse momentum. A key observable is the transverse mass

$$m_T^2 = 2 p_T^\ell p_T^{\rm miss} (1 - \cos \Delta\phi),$$

whose distribution is used in measurements of m_W.

2.6 Neutral currents: the photon and Z

The two neutral gauge fields before symmetry breaking are W^3_μ and B_μ. Their interaction with a fermion is

$$\mathcal{L}_{\text{neutral}} = -\bar{f}\gamma^\mu \left(gT_3W^3_\mu + g'YB_\mu\right) f. \tag{2.12}$$

Neither field alone is the photon. Define two orthogonal combinations,

$$A_\mu = s_W W^3_\mu + c_W B_\mu, \tag{2.13}$$

$$Z_\mu = c_W W^3_\mu - s_W B_\mu, \tag{2.14}$$

where $s_W = \sin\theta_W$ and $c_W = \cos\theta_W$. The inverse relations are

$$W^3_\mu = s_W A_\mu + c_W Z_\mu, \qquad B_\mu = c_W A_\mu - s_W Z_\mu.$$

Substituting into Eq. (2.12), the coefficient of A_μ is

$$g s_W T_3 + g' c_W Y.$$

The weak mixing angle is defined so that

$$e = g s_W = g' c_W. \tag{2.15}$$

The photon coefficient is therefore

$$e(T_3 + Y) = eQ,$$

and the electromagnetic interaction is

$$\boxed{\mathcal{L}_{\text{em}} = -eQ_f\bar{f}\gamma^\mu f A_\mu.} \tag{2.16}$$

For the orthogonal field, the coefficient is

$$\begin{aligned} g c_W T_3 - g' s_W Y &= \frac{g}{c_W}\left(c_W^2 T_3 - s_W^2 Y\right) \\ &= \frac{g}{c_W}\left[T_3 - s_W^2(T_3 + Y)\right] \\ &= \frac{g}{c_W}\left(T_3 - s_W^2 Q\right). \end{aligned}$$

Thus the chiral Z interaction is

$$\boxed{\mathcal{L}_Z = -\frac{g}{c_W}\bar{f}\gamma^\mu\left[\left(T_3^f - Q_f s_W^2\right)P_L - Q_f s_W^2 P_R\right] f Z_\mu.} \tag{2.17}$$

The photon coupling is the same for left- and right-handed components because they have the same electric charge. The Z coupling is generally different for the two chiralities because only the left-handed component has non-zero T_3. Vector and axial-vector couplings, decay widths and asymmetries will be developed in Lecture 4.

Experimental connection

The same neutral-current vertex is tested in $e^+e^- \to Z \to f\bar{f}$ and in Drell–Yan production $q\bar{q} \to \gamma^*/Z \to \ell^+\ell^-$. Total rates probe the coupling strengths, while angular asymmetries probe their chiral structure and provide precise determinations of the effective weak mixing angle.

2.7 What gauge symmetry predicts—and the remaining problem

Because $SU(2)_L$ is non-Abelian, its gauge bosons interact with one another. The gauge kinetic term predicts vertices such as $W^+W^-\gamma$ and W^+W^-Z, with strengths fixed by g and θ_W. Diboson measurements test this structure. The detailed field-strength algebra is not required for the remainder of this course.

There is, however, a crucial problem. The gauge theory constructed above describes massless gauge bosons and massless fermions. A direct vector mass term,

$$\frac{1}{2}m^2 W^a_\mu W^{a\mu},$$

is not invariant under a local non-Abelian gauge transformation. A direct Dirac mass,

$$-m_f \bar{f} f = -m_f(\bar{f}_L f_R + \bar{f}_R f_L),$$

is also forbidden before symmetry breaking because f_L and f_R transform in different electroweak representations.

We therefore need a mechanism that preserves the gauge structure of the Lagrangian while allowing the vacuum to hide part of the symmetry. A complex scalar doublet

$$\Phi = \begin{pmatrix} \phi^+ \\ \phi^0 \end{pmatrix} \sim (\mathbf{1}, \mathbf{2})_{1/2}$$

does exactly this. Its neutral component can acquire a vacuum expectation value without breaking electromagnetism. Lecture 3 will show in detail how this produces massive W and Z bosons, a massless photon, fermion masses and the physical Higgs boson.

2.8 Summary

The construction can be reduced to the following logical chain:

1. Observed charged-current transitions motivate left-handed doublets.
2. The transformations that mix the two entries form $SU(2)_L$.
3. Hypercharge $U(1)_Y$ is needed, with $Q = T_3 + Y$, to reproduce electric charges.
4. Local symmetry introduces four gauge fields through

$$D_\mu = \partial_\mu + igT^a W^a_\mu + ig' Y B_\mu.$$

5. W^1 and W^2 form $W^\pm$ and generate charged currents.
6. W^3 and B mix to form the photon and Z, with

$$e = g s_W = g' c_W.$$

7. Gauge invariance forbids explicit masses, leading to the Higgs mechanism.

Checkpoint

The four formulae to retain are

$$G_{\mathrm{EW}} = SU(2)_L \times U(1)_Y, \qquad Q = T_3 + Y,$$

$$D_\mu = \partial_\mu + igT^a W^a_\mu + ig' Y B_\mu, \qquad e = g s_W = g' c_W.$$

Everything else in the lecture explains how these statements produce the observed charged and neutral currents.

Short exercises

1. Use $Q = T_3 + Y$ to verify the charges of all fields in Eqs. (2.5) and (2.6).
2. Starting from $-g\bar{L}_L \gamma^\mu T^a L_L W^a_\mu$, derive Eq. (2.10), including the factor $1/\sqrt{2}$.
3. Substitute the neutral-field rotation into Eq. (2.12) and derive both the photon coupling eQ and the Z coupling in Eq. (2.17).

Chapter 3

Electroweak Symmetry Breaking and the Higgs Mechanism

The Higgs mechanism does not explicitly break gauge invariance. It allows the vacuum to hide part of the symmetry, while the Lagrangian retains the gauge structure needed for consistency at high energy.

Lecture 2 constructed the electroweak gauge theory from the group $SU(2)_L \times U(1)_Y$. Gauge invariance gave us the correct charged and neutral currents, but it also appeared to forbid precisely what nature requires: masses for the W and Z bosons and for the charged fermions. In this lecture we resolve that tension.

The central object is one complex scalar doublet. Its vacuum expectation value selects the electromagnetic direction $Q = T_3 + Y$ as the unbroken generator. Three scalar degrees of freedom are absorbed into the longitudinal polarisations of W^+, W^- and Z, while the fourth becomes the physical Higgs boson. We shall derive every gauge-boson mass and coupling rather than quote them, and then connect the results to muon decay, precision electroweak measurements and Higgs data.

3.1 What does spontaneous symmetry breaking mean?

A theory has a symmetry when its Lagrangian is unchanged by a transformation. The vacuum is the lowest-energy state of the theory. Spontaneous symmetry breaking occurs when the Lagrangian has a symmetry but the chosen vacuum does not. This distinction is essential: the equations retain the symmetry even though perturbation theory is organised around a state that hides it.

As a warm-up, consider one complex scalar field with a global $U(1)$ symmetry,

$$\phi(x) \longrightarrow e^{i\alpha}\phi(x), \tag{3.1}$$

and Lagrangian

$$\mathcal{L} = \partial_\mu\phi^*\partial^\mu\phi - V(\phi), \qquad V(\phi) = -\mu^2\phi^*\phi + \lambda(\phi^*\phi)^2, \tag{3.2}$$

where $\lambda > 0$. For $\mu^2 > 0$, the origin is not a minimum. The stationary condition gives

$$\frac{\partial V}{\partial(\phi^*\phi)} = -\mu^2 + 2\lambda\phi^*\phi = 0, \tag{3.3}$$

so the minima form a circle,

$$\phi^*\phi = \frac{\mu^2}{2\lambda} \equiv \frac{v^2}{2}. \tag{3.4}$$

Every point on this circle has the same energy. Choosing one, for example $\langle\phi\rangle = v/\sqrt{2}$, breaks the manifest rotational symmetry of the vacuum.

Parameterise fluctuations by

$$\phi(x) = \frac{1}{\sqrt{2}}\,[v + h(x) + i\pi(x)]. \tag{3.5}$$

Expanding the potential to quadratic order gives a massive radial mode and a massless angular mode,

$$m_h^2 = 2\lambda v^2 = 2\mu^2, \qquad m_\pi^2 = 0. \tag{3.6}$$

Moving radially changes $|\phi|$ and costs potential energy; moving tangentially along the circle of degenerate vacua does not. This geometrical observation is the content of Goldstone's theorem: for each spontaneously broken generator of a continuous *global* symmetry there is a massless scalar, a Goldstone boson.

Key idea

Spontaneous breaking is a statement about the vacuum, not an explicit deletion of terms from the Lagrangian. For a global symmetry the broken directions give physical massless Goldstone bosons. For a gauge symmetry the corresponding fields instead provide longitudinal vector-boson polarisations.

From global to gauge symmetry. For a global broken symmetry, the massless angular excitation is a physical Goldstone boson. In a gauge theory the corresponding degree of freedom instead becomes the longitudinal polarisation of a massive gauge field. The number of physical degrees of freedom is unchanged: a massless vector has two polarisations, whereas a massive vector has three. This observation is the essential content of the Higgs mechanism needed below.

3.2 The electroweak scalar sector

The minimal Standard Model contains one complex scalar doublet,

$$\Phi = \begin{pmatrix} \phi^+ \\ \phi^0 \end{pmatrix} \sim (\mathbf{1}, \mathbf{2})_{1/2}. \tag{3.7}$$

It contains four real degrees of freedom. The most general renormalisable $SU(2)_L \times U(1)_Y$ invariant potential is

$$V(\Phi) = -\mu^2 \Phi^\dagger\Phi + \lambda(\Phi^\dagger\Phi)^2, \qquad \lambda > 0. \tag{3.8}$$

When $\mu^2 > 0$, the minima satisfy

$$\Phi^\dagger\Phi = \frac{\mu^2}{2\lambda} \equiv \frac{v^2}{2}. \tag{3.9}$$

Many vacuum vectors satisfy this equation, but gauge transformations relate them. We choose the convenient representative

$$\langle\Phi\rangle = \frac{1}{\sqrt{2}}\begin{pmatrix} 0 \\ v \end{pmatrix}. \tag{3.10}$$

Why must the vacuum point in the neutral component? A charged vacuum would break electromagnetism and give the photon a mass, contrary to observation. The lower component has $T_3 = -1/2$ and $Y = +1/2$, and therefore

$$Q\langle\Phi\rangle = (T_3 + Y)\langle\Phi\rangle = 0. \tag{3.11}$$

Thus the generator Q leaves the vacuum invariant. The symmetry-breaking pattern is

$$SU(2)_L \times U(1)_Y \longrightarrow U(1)_{\text{em}}. \tag{3.12}$$

There are four electroweak generators and one unbroken generator, so three directions are broken. Correspondingly, three Goldstone degrees of freedom are available to become the longitudinal modes of W^+, W^- and Z. The one remaining scalar degree of freedom is physical.

A general useful parameterisation is

$$\Phi(x) = \exp\left(\frac{i\xi^a(x)\sigma^a}{v}\right) \frac{1}{\sqrt{2}} \begin{pmatrix} 0 \\ v + h(x) \end{pmatrix}. \tag{3.13}$$

In unitary gauge the fields ξ^a are removed from explicit expressions, leaving

$$\Phi(x) = \frac{1}{\sqrt{2}} \begin{pmatrix} 0 \\ v + h(x) \end{pmatrix}. \tag{3.14}$$

This form makes the physical particle content intuitive, although other gauges are often more convenient for loop calculations.

3.3 Deriving the gauge-boson masses

The complete result follows from one gauge-invariant term,

$$\mathcal{L}_\Phi = (D_\mu \Phi)^\dagger (D^\mu \Phi) - V(\Phi), \tag{3.15}$$

with

$$D_\mu = \partial_\mu + ig\frac{\sigma^a}{2} W_\mu^a + ig'\frac{1}{2} B_\mu. \tag{3.16}$$

To find masses we set $h = 0$ temporarily and act on the vacuum. Since the vacuum is constant,

$$D_\mu \langle \Phi \rangle = \frac{iv}{2\sqrt{2}} \begin{pmatrix} g(W_\mu^1 - iW_\mu^2) \\ -gW_\mu^3 + g'B_\mu \end{pmatrix}. \tag{3.17}$$

Therefore

$$(D_\mu \langle \Phi \rangle)^\dagger (D^\mu \langle \Phi \rangle) = \frac{v^2}{8} \left[g^2((W^1)^2 + (W^2)^2) + (gW^3 - g'B)^2 \right]. \tag{3.18}$$

3.3.1 The charged sector

Using

$$W_\mu^\pm = \frac{W_\mu^1 \mp iW_\mu^2}{\sqrt{2}}, \qquad (W^1)^2 + (W^2)^2 = 2W_\mu^+ W^{-\mu}, \tag{3.19}$$

the charged part becomes

$$\mathcal{L}_{\text{mass}}^{\text{charged}} = \frac{g^2 v^2}{4} W_\mu^+ W^{-\mu}. \tag{3.20}$$

Comparing with $m_W^2 W_\mu^+ W^{-\mu}$ gives

$$\boxed{m_W = \frac{gv}{2}.} \tag{3.21}$$

The two real gauge fields W^1 and W^2 combine into one complex charged field and its conjugate. They necessarily have equal masses.

3.3.2 The neutral sector

The neutral mass terms can be written as

$$\mathcal{L}_{\text{mass}}^{\text{neutral}} = \frac{1}{2}\begin{pmatrix} W_\mu^3 & B_\mu \end{pmatrix} \frac{v^2}{4}\begin{pmatrix} g^2 & -gg' \\ -gg' & g'^2 \end{pmatrix}\begin{pmatrix} W^{3\mu} \\ B^\mu \end{pmatrix}. \tag{3.22}$$

The determinant of this matrix vanishes,

$$\det\begin{pmatrix} g^2 & -gg' \\ -gg' & g'^2 \end{pmatrix} = 0, \tag{3.23}$$

so one neutral eigenstate is exactly massless. This is not an accident or a fine tuning: it follows from the unbroken generator in Eq. (3.11).

Define the weak mixing angle by

$$s_W \equiv \sin\theta_W = \frac{g'}{\sqrt{g^2+g'^2}}, \qquad c_W \equiv \cos\theta_W = \frac{g}{\sqrt{g^2+g'^2}}, \tag{3.24}$$

or equivalently $\tan\theta_W = g'/g$. The orthogonal rotation

$$\begin{pmatrix} Z_\mu \\ A_\mu \end{pmatrix} = \begin{pmatrix} c_W & -s_W \\ s_W & c_W \end{pmatrix}\begin{pmatrix} W_\mu^3 \\ B_\mu \end{pmatrix} \tag{3.25}$$

diagonalises the matrix. The eigenvalues give

$$\boxed{m_Z = \frac{v}{2}\sqrt{g^2+g'^2}}, \qquad \boxed{m_A = 0}. \tag{3.26}$$

It follows immediately that

$$\boxed{m_W = m_Z c_W} \tag{3.27}$$

at tree level. The same rotation found from the mass matrix also gives the electromagnetic coupling relation

$$e = g s_W = g' c_W. \tag{3.28}$$

Thus mass mixing and charge universality are two aspects of the same symmetry- breaking structure.

Checkpoint

Do not interpret A_μ as a field that “failed to acquire mass by chance.” It is massless because its generator Q leaves the Higgs vacuum invariant. Conversely, a generator that changes the vacuum corresponds to a massive gauge field.

3.4 The electroweak scale from muon decay

The low-energy charged-current relation from Lecture 1 is

$$\frac{G_F}{\sqrt{2}} = \frac{g^2}{8m_W^2}. \tag{3.29}$$

Using $m_W = gv/2$, the gauge coupling cancels:

$$\frac{G_F}{\sqrt{2}} = \frac{1}{2v^2}. \tag{3.30}$$

Consequently,

$$\boxed{v = (\sqrt{2}G_F)^{-1/2} \simeq 246 \text{ GeV}.} \tag{3.31}$$

This is a beautiful bridge between low- and high-energy physics. A precision measurement of the muon lifetime fixes the vacuum expectation value governing W and Z masses and all Standard Model Higgs couplings. The quantity $v/\sqrt{2} \simeq 174$ GeV is also frequently encountered, particularly in fermion mass formulae; it should not be confused with v itself.

Another important tree-level prediction is the rho parameter,

$$\rho \equiv \frac{m_W^2}{m_Z^2 c_W^2} = 1. \tag{3.32}$$

For one Higgs doublet this equality follows from an approximate global custodial symmetry of the scalar sector. Radiative corrections, especially those sensitive to the top–bottom mass splitting, shift ρ away from one. Precision measurements of m_W, m_Z and neutral-current observables are therefore sensitive to heavy virtual particles and to non-standard Higgs representations.

Experimental connection

The input G_F comes from muon decay at energies of order the muon mass, whereas m_W and m_Z are measured through resonant production at colliders. Testing their relation requires radiative corrections and a carefully defined renormalisation scheme. Agreement across these very different scales is a major quantitative success of the electroweak theory.

3.5 The physical Higgs boson

In unitary gauge, substitute Eq. (3.14) into the potential. The minimum condition $\mu^2 = \lambda v^2$ removes the term linear in h. Up to an irrelevant constant,

$$V(h) = \frac{1}{2}m_h^2 h^2 + \frac{m_h^2}{2v}h^3 + \frac{m_h^2}{8v^2}h^4, \qquad \boxed{m_h^2 = 2\lambda v^2.} \tag{3.33}$$

The Higgs mass determines the quartic coupling at the electroweak scale,

$$\lambda = \frac{m_h^2}{2v^2} \simeq 0.13 \tag{3.34}$$

for a Higgs mass near 125 GeV. The cubic and quartic self-interactions are therefore predictions once m_h and v are fixed. Measuring them tests the shape of the Higgs potential rather than merely the existence of a scalar resonance.

Keeping h in the scalar kinetic term replaces v^2 in the mass terms by $(v+h)^2$. Hence

$$\begin{aligned} \mathcal{L} \supset\ & m_W^2 W_\mu^+ W^{-\mu}\left(1 + \frac{2h}{v} + \frac{h^2}{v^2}\right) \\ & + \frac{1}{2}m_Z^2 Z_\mu Z^\mu \left(1 + \frac{2h}{v} + \frac{h^2}{v^2}\right). \end{aligned} \tag{3.35}$$

The coefficients show that the Higgs coupling to a vector boson is controlled by that boson's mass:

$$g_{hWW} = \frac{2m_W^2}{v}, \qquad g_{hZZ} = \frac{2m_Z^2}{v}, \tag{3.36}$$

where the second expression refers to the conventional Feynman-rule normalisation including the identical Z fields. There are also $hhWW$ and $hhZZ$ contact interactions fixed by the same expansion.

The Yukawa Lagrangian gives, in the fermion mass basis,

$$\mathcal{L}_Y \supset -m_f \bar{f} f - \frac{m_f}{v} h \bar{f} f, \tag{3.37}$$

so

$$\boxed{g_{hff} = \frac{m_f}{v}.} \tag{3.38}$$

The Standard Model therefore predicts a striking pattern: the Higgs couples most strongly to the heaviest particles. This is why Higgs production is dominated by top-quark effects even though an on-shell Higgs cannot decay into a top pair, and why decays to $b\bar{b}$, WW^* and ZZ^* are central experimental channels.

At tree level the fermionic partial width, neglecting radiative corrections, is

$$\Gamma(h \to f\bar{f}) = N_c \frac{m_h m_f^2}{8\pi v^2} \left(1 - \frac{4m_f^2}{m_h^2}\right)^{3/2}, \tag{3.39}$$

where $N_c = 3$ for quarks and 1 for leptons. The factor m_f^2 is a direct consequence of the Yukawa coupling. In practice, QCD corrections and the running quark mass are essential for precision predictions.

The decays $h \to gg$ and $h \to \gamma\gamma$ are absent at tree level because the Higgs is colourless and electrically neutral. They arise through loops, predominantly a top loop for gg and interfering W- and top-loop contributions for $\gamma\gamma$. These loop-induced channels illustrate how the Higgs can probe particles heavier than itself and possible new charged or coloured states.

Experimental connection

Experimental Higgs measurements are often expressed through signal strengths,

$$\mu_{i\to h\to f} = \frac{\sigma_i \, \mathrm{BR}_f}{(\sigma_i \, \mathrm{BR}_f)_{\mathrm{SM}}}.$$

Different production modes—gluon fusion, vector-boson fusion, associated Vh production and $t\bar{t}h$—separate different couplings. Agreement of many such measurements with the mass-proportional pattern is evidence that the observed scalar participates in electroweak symmetry breaking.

3.6 Fermion masses and the remaining flavour puzzle

Gauge-invariant Yukawa interactions connect a left-handed doublet, the Higgs field and a right-handed singlet. After replacing the neutral Higgs component by $(v + h)/\sqrt{2}$, they give

$$m_f = \frac{y_f v}{\sqrt{2}}, \qquad \mathcal{L}_{hff} = -\frac{m_f}{v} h \bar{f} f. \tag{3.40}$$

Thus the same parameter determines a fermion mass and its Higgs coupling. For three generations the Yukawa couplings are matrices, and their misalignment produces CKM mixing. Lecture 5 develops this in detail.

The Higgs mechanism explains how fermions can acquire gauge-invariant masses; it does not explain why the Yukawa couplings span many orders of magnitude or why quark mixing has its observed pattern.

3.7 What the mechanism predicts

Once v, the gauge couplings and m_h are specified, the minimal Standard Model relates m_W, m_Z, Higgs couplings and the scalar self-coupling. Radiative corrections systematically modify the tree-level relations, making precision measurements sensitive to virtual heavy particles. The most direct experimental tests are measurements of Higgs production and decay rates, especially whether couplings follow the predicted mass-proportional pattern.

3.8 Putting the pieces together: the electroweak Lagrangian

It is useful to pause here and assemble the ingredients that have so far been introduced separately. The Yukawa interactions are not generated by the Higgs potential or by the gauge kinetic terms. They form an additional, independently allowed sector of the most general renormalisable Lagrangian consistent with the Standard Model gauge symmetry.

Before electroweak symmetry breaking, the electroweak Lagrangian can be organised as

$$\boxed{\mathcal{L}_{\text{EW}} = \mathcal{L}_{\text{gauge}} + \mathcal{L}_{\text{fermion}} + \mathcal{L}_{\text{Higgs}} + \mathcal{L}_{\text{Yukawa}}} \tag{3.41}$$

where

$$\begin{aligned}
\mathcal{L}_{\text{gauge}} &= -\frac{1}{4}W^a_{\mu\nu}W^{a\mu\nu} - \frac{1}{4}B_{\mu\nu}B^{\mu\nu}, && (3.42)\\
\mathcal{L}_{\text{fermion}} &= \sum_{\psi=Q_L,L_L,u_R,d_R,e_R} i\overline{\psi}\gamma^\mu D_\mu\psi, && (3.43)\\
\mathcal{L}_{\text{Higgs}} &= (D_\mu\Phi)^\dagger(D^\mu\Phi) - V(\Phi), \qquad V(\Phi) = -\mu^2\Phi^\dagger\Phi + \lambda(\Phi^\dagger\Phi)^2, && (3.44)\\
\mathcal{L}_{\text{Yukawa}} &= -\overline{Q}_L Y_d \Phi d_R - \overline{Q}_L Y_u \widetilde{\Phi} u_R - \overline{L}_L Y_e \Phi e_R + \text{h.c.}, \qquad \widetilde{\Phi} = i\sigma^2\Phi^*. && (3.45)
\end{aligned}$$

Generation indices and the sum over the three generations are implicit.

The gauge-field strengths contain the kinetic terms of the gauge bosons. The non-Abelian $SU(2)_L$ field strength also generates interactions among the weak gauge bosons themselves. The covariant derivatives in $\mathcal{L}_{\text{fermion}}$ and $\mathcal{L}_{\text{Higgs}}$ generate the interactions of matter and the Higgs field with W^a_μ and B_μ. Their form is fixed by the gauge representations and hypercharges of the fields.

The Higgs sector contains both the scalar potential and the interaction that generates the W- and Z-boson masses. The Yukawa sector is separate from the Higgs potential. It contains all renormalisable gauge-invariant interactions that connect left-handed fermion doublets to right-handed fermion singlets through the Higgs field. The Yukawa matrices Y_u, Y_d and Y_e are independent dimensionless parameters of the Standard Model.

After electroweak symmetry breaking, choose unitary gauge:

$$\Phi(x) = \frac{1}{\sqrt{2}}\begin{pmatrix} 0 \\ v + h(x) \end{pmatrix}, \qquad \widetilde{\Phi}(x) = \frac{1}{\sqrt{2}}\begin{pmatrix} v + h(x) \\ 0 \end{pmatrix}. \tag{3.46}$$

The replacement of the neutral Higgs component by $(v+h)/\sqrt{2}$ reorganises the gauge-basis Lagrangian into the particle language used by experiments.

From the Higgs kinetic term,

$$(D_\mu\Phi)^\dagger(D^\mu\Phi), \tag{3.47}$$

we obtain the masses of the weak gauge bosons,

$$m_W = \frac{gv}{2}, \qquad m_Z = \frac{v}{2}\sqrt{g^2 + g'^2}, \qquad m_A = 0, \tag{3.48}$$

as well as the interactions of the physical Higgs boson with $W^\pm$ and Z.

From the Yukawa sector we obtain the fermion mass matrices,

$$M_f = \frac{v}{\sqrt{2}} Y_f, \qquad f = u, d, e. \tag{3.49}$$

For example,

$$\mathcal{L}_{\text{Yukawa}} \supset -\overline{f}_L M_f f_R - \frac{h}{v}\overline{f}_L M_f f_R + \text{h.c.} \tag{3.50}$$

After diagonalising the fermion mass matrices, this becomes

$$\mathcal{L}_{\text{Yukawa}} \supset -\sum_f m_f \overline{f} f - \sum_f \frac{m_f}{v} h \overline{f} f. \tag{3.51}$$

Thus the same Yukawa coupling determines both a fermion mass and its interaction with the physical Higgs boson:

$$m_f = \frac{y_f v}{\sqrt{2}}, \qquad g_{hff} = \frac{m_f}{v}. \tag{3.52}$$

The up- and down-quark mass matrices are generally diagonalised by different rotations. The mismatch between their left-handed rotations appears in the charged weak current as the CKM matrix. Electroweak symmetry breaking therefore does more than generate masses: it converts the gauge-basis Lagrangian into a mass-basis theory containing $W^\pm$, Z, the photon, the physical Higgs boson, massive fermions and flavour mixing.

Gauge-fixing and ghost terms must also be added when quantising the theory. They are not displayed in Eq. (3.41), since they do not introduce new physical parameters or asymptotic particles and are not needed for the tree-level phenomenology discussed here.

Checkpoint

The transition from the symmetric electroweak theory to measurable phenomenology can be summarised as

$$\mathcal{L}_{\text{EW}} \xrightarrow{\langle\Phi\rangle\neq 0} \begin{cases} m_W,\ m_Z,\ m_A = 0, \\ m_f = Y_f v/\sqrt{2}, \\ hWW,\ hZZ,\ h\overline{f}f \text{ interactions}, \\ \text{charged and neutral weak currents}, \\ \text{flavour mixing through the CKM matrix.} \end{cases}$$

Lecture 4 starts from this broken-phase Lagrangian and uses its vertices to predict decay widths, cross sections and asymmetries.

3.9 Summary

The scalar potential has a continuum of degenerate minima. Choosing a vacuum with

$$\langle\Phi\rangle = \frac{1}{\sqrt{2}}(0, v)^T \tag{3.53}$$

hides $SU(2)_L \times U(1)_Y$ while leaving the electromagnetic generator $Q = T_3 + Y$ unbroken. Three Goldstone degrees of freedom become the longitudinal polarisations of W^+, W^- and Z. One physical scalar remains.

The scalar kinetic term gives

$$m_W = \frac{gv}{2}, \qquad m_Z = \frac{v}{2}\sqrt{g^2 + g'^2}, \qquad m_A = 0, \tag{3.54}$$

and therefore $m_W = m_Z c_W$ at tree level. Muon decay fixes

$$v = (\sqrt{2}G_F)^{-1/2} \simeq 246 \text{ GeV}. \tag{3.55}$$

The remaining scalar has $m_h^2 = 2\lambda v^2$ and couplings

$$g_{hVV} \propto \frac{m_V^2}{v}, \qquad g_{hff} = \frac{m_f}{v}. \tag{3.56}$$

Checkpoint

The Higgs mechanism should be remembered as a chain of logic:

$$\text{gauge-invariant scalar dynamics} \longrightarrow \langle\Phi\rangle \neq 0 \longrightarrow SU(2)_L \times U(1)_Y \to U(1)_{\text{em}}$$

$$\longrightarrow \quad m_W, m_Z \neq 0, \quad m_A = 0, \quad \text{three longitudinal modes plus one physical Higgs.}$$

Short exercises

1. Starting from Eq. (3.8), derive $v^2 = \mu^2/\lambda$ and $m_h^2 = 2\lambda v^2$.
2. Act with $Q = T_3 + Y$ on the vacuum in Eq. (3.10). Why does electromagnetism remain unbroken?
3. Use the Pauli matrices to derive Eq. (3.17) and obtain m_W.
4. Diagonalise the neutral mass matrix in Eq. (3.22) and identify the photon and Z.

Chapter 4

Electroweak Phenomenology and Precision Tests

A Lagrangian becomes physics only when we learn how its parameters and symmetries appear in measurable rates, distributions and asymmetries.

At the end of Lecture 3 we assembled the complete electroweak Lagrangian from its gauge, fermion, Higgs and Yukawa sectors. After replacing the Higgs field by its vacuum value plus the physical fluctuation, that one Lagrangian gives the mass eigenstates $W^{\pm}$, Z, A and h, together with their couplings to quarks and leptons. The Yukawa sector supplies fermion masses and Higgs couplings, while the fermion kinetic terms supply the charged and neutral gauge currents studied below.

We now change viewpoint: instead of constructing the theory, we use its mass-basis vertices to predict measurable quantities. The practical chain is

$$\boxed{\text{electroweak Lagrangian} \longrightarrow \text{vertex} \longrightarrow \mathcal{M} \longrightarrow \Gamma,\ \sigma,\ \text{asymmetry}} \tag{4.1}$$

The emphasis is not on memorising a catalogue of cross sections. Instead, we will learn a reusable strategy: identify the relevant current, calculate the amplitude, expose the chiral couplings, and then choose an observable that isolates the desired combination of parameters.

The W and Z bosons are simultaneously particles that can be produced on shell and mediators of low-energy interactions. Their masses, widths, branching fractions and angular distributions overconstrain the theory. Quantum loop corrections then turn this overconstrained system into an indirect microscope for heavy particles and possible new physics.

The sections after section 4.3 in this chapter are optional and for self-study purpose and won't be delivered during the lecture.

4.1 The electroweak interactions in the mass basis

After symmetry breaking, the charged-current interaction is

$$\mathcal{L}_{\rm cc} = -\frac{g}{\sqrt{2}}\left[J_+^{\mu}W_{\mu}^{+} + J_-^{\mu}W_{\mu}^{-}\right], \tag{4.2}$$

where

$$J_+^{\mu} = \sum_{\ell}\bar{\nu}_{\ell L}\gamma^{\mu}\ell_L + \sum_{i,j}\bar{u}_{Li}\gamma^{\mu}V_{ij}d_{Lj}, \qquad J_-^{\mu} = (J_+^{\mu})^{\dagger}. \tag{4.3}$$

Every term is left handed. The same coupling g controls leptonic and quark vertices, while the CKM element V_{ij} determines the strength of a particular quark-flavour transition.

The neutral-current interaction is

$$\mathcal{L}_Z = -\frac{g}{2c_W} \sum_f \bar{f}\gamma^\mu (g_V^f - g_A^f \gamma^5) f Z_\mu, \tag{4.4}$$

with

$$g_V^f = T_3^f - 2Q_f s_W^2, \qquad g_A^f = T_3^f. \tag{4.5}$$

Electromagnetism is described by

$$\mathcal{L}_{\text{em}} = -e \sum_f Q_f \bar{f}\gamma^\mu f A_\mu. \tag{4.6}$$

The photon coupling is purely vector-like, whereas the Z has both vector and axial pieces. Parity-violating observables are therefore especially clean probes of Z exchange.

It is sometimes more intuitive to define left- and right-handed couplings,

$$g_L^f = T_3^f - Q_f s_W^2, \qquad g_R^f = -Q_f s_W^2, \tag{4.7}$$

so that $g_V = g_L + g_R$ and $g_A = g_L - g_R$. Different papers distribute factors of two differently between the prefactor and these definitions. A reliable calculation should begin by stating the Lagrangian convention, rather than copying a coupling from a table without its normalisation.

Key idea

Rates mainly measure sums of squared couplings, while asymmetries measure differences or interference. Combining them separates left- and right-handed interactions much more effectively than either class of observable alone.

4.2 From the electroweak Lagrangian to Feynman diagrams

A Feynman diagram is a graphical instruction for constructing a quantum amplitude. It is not itself an observable. The practical sequence is

$$\boxed{\mathcal{L}_{\text{int}} \longrightarrow \text{Feynman rules} \longrightarrow \text{Feynman diagrams} \longrightarrow \mathcal{M} \longrightarrow \overline{|\mathcal{M}|^2} \longrightarrow \Gamma \text{ or } \sigma}. \tag{4.8}$$

This section summarises the electroweak Feynman rules needed in this lecture and illustrates how they are used to calculate a matrix element.

4.2.1 From an interaction term to a vertex

In the conventions used here, a vertex factor is obtained by multiplying the coefficient of the corresponding fields in the interaction Lagrangian by i, while retaining its spinor, Lorentz, flavour and internal-symmetry structure.

For example, the charged-current interaction contains

$$\mathcal{L}_{\text{cc}} \supset -\frac{g}{\sqrt{2}} \bar{\ell}\gamma^\mu P_L \nu_\ell W_\mu^- + \text{h.c.}, \qquad P_L = \frac{1-\gamma^5}{2}. \tag{4.9}$$

The corresponding $W^-\ell^-\bar{\nu}_\ell$ vertex factor is therefore

$$\boxed{-i\frac{g}{\sqrt{2}}\gamma^\mu P_L}. \tag{4.10}$$

The factor P_L shows explicitly that the charged weak interaction couples only to left-handed fermions and right-handed antifermions. An overall phase of a single amplitude has no effect on an observable, but relative signs between diagrams that interfere must be treated consistently.

4.2.2 External particles and internal lines

Each external particle contributes a wavefunction:

External state	Wavefunction
Incoming fermion	$u(p,s)$
Outgoing fermion	$\overline{u}(p,s)$
Incoming antifermion	$\overline{v}(p,s)$
Outgoing antifermion	$v(p,s)$
Incoming vector boson	$\epsilon_\mu(p,\lambda)$
Outgoing vector boson	$\epsilon^*_\mu(p,\lambda)$

Here p is the four-momentum, s labels a fermion spin state, and λ labels a vector-boson polarisation.

An internal line contributes a propagator. For example, a fermion propagator is

$$\frac{i(\not{q}+m_f)}{q^2-m_f^2+i\epsilon}, \tag{4.11}$$

where q is the four-momentum carried by the internal line.

In Feynman gauge, the propagators of a massive weak boson and the photon are

$$\frac{-ig_{\mu\nu}}{q^2-m_V^2+i\epsilon}, \qquad V=W,Z, \tag{4.12}$$

and

$$\frac{-ig_{\mu\nu}}{q^2+i\epsilon}, \tag{4.13}$$

respectively. Individual propagators and diagrams can depend on the gauge choice, but the complete prediction for a physical observable is gauge independent.

4.2.3 Electroweak fermion vertices

The principal electroweak fermion vertices are

$$W^-_\mu\,\ell^-\,\overline{\nu}_\ell: \qquad -i\frac{g}{\sqrt{2}}\gamma^\mu P_L, \tag{4.14}$$

$$W^+_\mu\,u_i\,\overline{d}_j: \qquad -i\frac{g}{\sqrt{2}}V_{ij}\gamma^\mu P_L, \tag{4.15}$$

$$W^-_\mu\,d_j\,\overline{u}_i: \qquad -i\frac{g}{\sqrt{2}}V^*_{ij}\gamma^\mu P_L, \tag{4.16}$$

$$Z_\mu\,f\,\overline{f}: \qquad -i\frac{g}{2c_W}\gamma^\mu\left(g_V^f-g_A^f\gamma^5\right), \tag{4.17}$$

$$A_\mu\,f\,\overline{f}: \qquad -ieQ_f\gamma^\mu, \tag{4.18}$$

$$h\,f\,\overline{f}: \qquad -i\frac{m_f}{v}. \tag{4.19}$$

Here

$$c_W=\cos\theta_W, \qquad s_W=\sin\theta_W, \tag{4.20}$$

and

$$g_V^f=T_3^f-2Q_fs_W^2, \qquad g_A^f=T_3^f. \tag{4.21}$$

The quantities T_3^f and Q_f are the third component of weak isospin and the electric charge of the fermion. The matrix element V_{ij} is an element of the CKM quark-mixing matrix.

The photon vertex is purely vector-like. The Z vertex contains both vector and axial-vector couplings, while the W vertex contains the left-handed projector P_L.

4.2.4 Worked example: leptonic W decay

Consider the decay

$$W^-(q,\lambda) \longrightarrow \ell^-(p_1,s_1) + \overline{\nu}_\ell(p_2,s_2), \qquad q = p_1 + p_2. \tag{4.22}$$

The corresponding tree-level Feynman diagram is

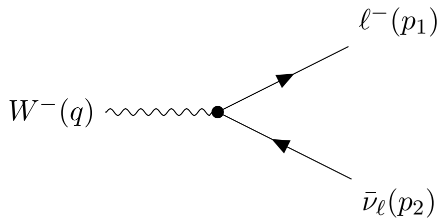

Tree-level decay $W^- \to \ell^-\bar{\nu}_\ell$.

The incoming W^- contributes a polarisation vector $\epsilon_\mu(q,\lambda)$. The outgoing charged lepton contributes $\overline{u}_\ell(p_1,s_1)$, while the outgoing antineutrino contributes $v_\nu(p_2,s_2)$. The interaction vertex contributes

$$-i\frac{g}{\sqrt{2}}\gamma^\mu P_L. \tag{4.23}$$

Combining these factors gives

$$i\mathcal{M} = \overline{u}_\ell(p_1)\left(-i\frac{g}{\sqrt{2}}\gamma^\mu P_L\right) v_\nu(p_2)\,\epsilon_\mu(q). \tag{4.24}$$

Removing the common factor of i, the invariant amplitude is

$$\boxed{\mathcal{M} = -\frac{g}{\sqrt{2}}\overline{u}_\ell(p_1)\gamma^\mu P_L v_\nu(p_2)\,\epsilon_\mu(q)}. \tag{4.25}$$

This expression is therefore not a separate assumption: it follows directly from the charged-current interaction in the electroweak Lagrangian.

4.2.5 Spin and polarisation sums

The decay rate depends on the squared amplitude. When final-state spins are not observed, we sum over them. The relevant spin-sum identities are

$$\sum_s u(p,s)\overline{u}(p,s) = p + m, \qquad \sum_s v(p,s)\overline{v}(p,s) = p - m. \tag{4.26}$$

For a massive vector boson,

$$\sum_{\lambda=1}^{3} \epsilon_\mu^{(\lambda)}(q)\epsilon_\nu^{(\lambda)*}(q) = -g_{\mu\nu} + \frac{q_\mu q_\nu}{m_V^2}. \tag{4.27}$$

A massive vector boson has three physical polarisations: two transverse and one longitudinal.

For an unpolarised W sample, we average over its three initial polarisations. Neglecting the lepton and neutrino masses,

$$\begin{aligned}\overline{|\mathcal{M}|^2} = \frac{1}{3}\frac{g^2}{2}&\left(-g_{\mu\nu} + \frac{q_\mu q_\nu}{m_W^2}\right)\\ &\times \mathrm{Tr}\left[p_1\gamma^\mu P_L p_2 \gamma^\nu P_L\right]. \end{aligned} \tag{4.28}$$

Using

$$q^2 = m_W^2, \qquad p_1^2 = p_2^2 = 0, \qquad 2p_1 \cdot p_2 = m_W^2, \tag{4.29}$$

the trace gives

$$\boxed{\overline{|\mathcal{M}|^2} = \frac{g^2 m_W^2}{3}}. \tag{4.30}$$

For two massless final particles,

$$\Gamma = \frac{\overline{|\mathcal{M}|^2}}{16\pi m_W}. \tag{4.31}$$

The leptonic partial width is therefore

$$\Gamma(W \to \ell\nu) = \frac{g^2 m_W}{48\pi}. \tag{4.32}$$

Using

$$\frac{G_F}{\sqrt{2}} = \frac{g^2}{8m_W^2}, \tag{4.33}$$

we obtain

$$\boxed{\Gamma(W \to \ell\nu) = \frac{G_F m_W^3}{6\pi\sqrt{2}}}. \tag{4.34}$$

4.2.6 Z-boson decay

The decay of a Z boson into a fermion–antifermion pair is represented by

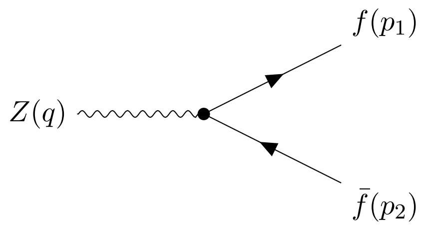

Tree-level decay $Z \to f\bar{f}$.

The $Zf\bar{f}$ vertex gives

$$i\mathcal{M} = \overline{u}_f(p_1)\left[-i\frac{g}{2c_W}\gamma^\mu\left(g_V^f - g_A^f\gamma^5\right)\right]v_f(p_2)\,\epsilon_\mu(q). \tag{4.35}$$

Thus

$$\boxed{\mathcal{M} = -\frac{g}{2c_W}\overline{u}_f(p_1)\gamma^\mu\left(g_V^f - g_A^f\gamma^5\right)v_f(p_2)\,\epsilon_\mu(q)}. \tag{4.36}$$

The simultaneous presence of g_V^f and g_A^f produces parity violation and leads to the angular asymmetries discussed later in this lecture.

4.2.7 Scattering example: $e^+e^- \to f\bar{f}$

The process

$$e^-(p_1) + e^+(p_2) \longrightarrow f(k_1) + \bar{f}(k_2) \tag{4.37}$$

receives both photon- and Z-exchange contributions.

The photon-exchange diagram is

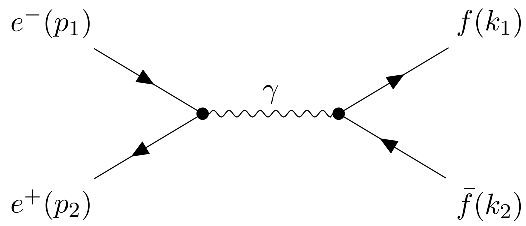

Photon exchange in $e^+e^- \to f\bar{f}$.

The corresponding photon-exchange amplitude is

$$i\mathcal{M}_\gamma = \overline{v}_e(p_2)\,(-ieQ_e\gamma^\mu)\,u_e(p_1)\frac{-ig_{\mu\nu}}{s} \times \overline{u}_f(k_1)\,(-ieQ_f\gamma^\nu)\,v_f(k_2), \tag{4.38}$$

where

$$s = (p_1 + p_2)^2 \tag{4.39}$$

is the square of the centre-of-mass energy.

The Z-exchange diagram has the same topology:

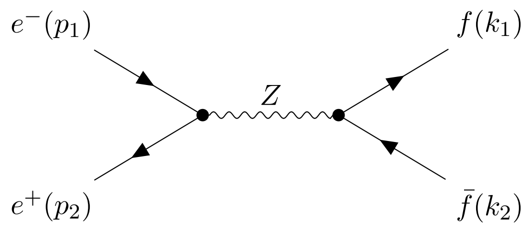

Z-boson exchange in $e^+e^- \to f\bar{f}$.

Its amplitude contains the Z propagator,

$$\frac{-ig_{\mu\nu}}{s - m_Z^2 + im_Z\Gamma_Z}, \tag{4.40}$$

and a $Zf\bar{f}$ vertex at either end. The width Γ_Z is included near the resonance because the Z is unstable.

Since both diagrams connect the same initial and final states, the amplitudes must be added before squaring:

$$\mathcal{M} = \mathcal{M}_\gamma + \mathcal{M}_Z. \tag{4.41}$$

Therefore,

$$|\mathcal{M}|^2 = |\mathcal{M}_\gamma|^2 + |\mathcal{M}_Z|^2 + 2\,\mathrm{Re}\,(\mathcal{M}_\gamma\mathcal{M}_Z^*)\,. \tag{4.42}$$

The final term represents photon–Z interference. It is particularly important away from the exact Z pole and contributes to parity-violating angular asymmetries.

4.2.8 From a scattering amplitude to a cross section

For a general process

$$1 + 2 \longrightarrow 3 + \cdots + n, \tag{4.43}$$

the differential cross section is

$$d\sigma = \frac{\overline{|\mathcal{M}|^2}\, d\Phi_{n-2}}{4\sqrt{(p_1 \cdot p_2)^2 - m_1^2 m_2^2}}. \tag{4.44}$$

The denominator is the incident flux factor. For a two-to-two process in the centre-of-mass frame,

$$\frac{d\sigma}{d\Omega} = \frac{1}{64\pi^2 s} \frac{|\mathbf{p}_f|}{|\mathbf{p}_i|} \overline{|\mathcal{M}|^2}, \tag{4.45}$$

where $|\mathbf{p}_i|$ and $|\mathbf{p}_f|$ are the magnitudes of the initial- and final-state three-momenta.

Key idea

A Feynman diagram is a graphical instruction for constructing an amplitude. External lines provide wavefunctions, internal lines provide propagators, and interaction points provide vertex factors. Amplitudes for indistinguishable alternatives must be added coherently before calculating $|\mathcal{M}|^2$ and integrating over phase space.

4.3 Decay widths: turning vertices into observables

For an unstable particle of mass M, the differential decay width into n particles is

$$d\Gamma = \frac{1}{2M} \overline{|\mathcal{M}|^2}\, d\Phi_n. \tag{4.46}$$

Here $\mathcal{M}$ is the invariant decay amplitude. The bar denotes a sum over final spins and colours and, for an unpolarised parent, an average over its spin or polarisation states. The Lorentz-invariant phase-space element is

$$d\Phi_n = (2\pi)^4 \delta^{(4)}\left(p - \sum_{i=1}^{n} p_i\right) \prod_{i=1}^{n} \frac{d^3\mathbf{p}_i}{(2\pi)^3, 2E_i}, \tag{4.47}$$

where p is the parent four-momentum, $p_i = (E_i, \mathbf{p}_i)$ are the final-state four-momenta, and the delta function enforces energy–momentum conservation.

For a two-body decay $X(M) \to 1(m_1) + 2(m_2)$, the magnitude of either three-momentum in the rest frame of X is

$$|\mathbf{p}| = \frac{1}{2M} \lambda^{1/2}(M^2, m_1^2, m_2^2), \qquad \lambda(x, y, z) = x^2 + y^2 + z^2 - 2xy - 2xz - 2yz. \tag{4.48}$$

If $m_1, m_2 \ll M$, then $|\mathbf{p}| = M/2$. After angular integration,

$$\boxed{\Gamma = \frac{\overline{|\mathcal{M}|^2}}{16\pi M}} \tag{4.49}$$

when the spin-summed and polarisation-averaged squared amplitude has no remaining angular dependence.

4.3.1 Why weak widths contain $G_F M^3$

The Fermi constant G_F is determined very accurately from the muon lifetime. At momenta much smaller than m_W, the virtual W propagator behaves as $1/m_W^2$. Two charged-current vertices supply two factors of $g/\sqrt{2}$. Matching the resulting low-energy amplitude for $\mu^- \to e^-\bar{\nu}_e\nu_\mu$ to Fermi's four-fermion theory gives

$$\boxed{\frac{G_F}{\sqrt{2}} = \frac{g^2}{8m_W^2}}, \qquad g^2 = 4\sqrt{2}\, G_F m_W^2. \tag{4.50}$$

Thus G_F is not an additional interaction inserted into an on-shell W decay: it is a convenient, precisely measured way of expressing the same weak gauge coupling g.

The powers of mass can now be understood without detailed algebra. Fermion spin sums give $\overline{|\mathcal{M}|^2} \sim g^2M^2$, and two-body phase space then gives $\Gamma \sim g^2M$. Replacing g^2 through Eq. (4.50) supplies two further powers of the weak-boson mass:

$$\Gamma \sim g^2M \sim G_F M^3. \tag{4.51}$$

This also follows from dimensional analysis in natural units: $[G_F] = M^{-2}$ and $[\Gamma] = M$, so G_FM^3 has the required dimension.

4.3.2 Leptonic W decay

Consider

$$W^-(q) \to \ell^-(p_1)\bar{\nu}_\ell(p_2), \qquad q = p_1 + p_2, \tag{4.52}$$

where q, p_1 and p_2 denote the corresponding four-momenta. Neglecting the charged-lepton and neutrino masses, the charged-current vertex gives

$$\mathcal{M} = -\frac{g}{\sqrt{2}}\,\bar{u}_\ell(p_1)\gamma^\mu P_L v_\nu(p_2)\,\epsilon_\mu(q), \qquad P_L = \frac{1-\gamma^5}{2}. \tag{4.53}$$

u_ℓ and v_ν are the outgoing lepton and antineutrino spinors, ϵ_μ is the W polarisation vector, and P_L selects the left-handed weak current. A massive vector boson has three polarisations, with

$$\sum_{\lambda=1}^{3} \epsilon_\mu^{(\lambda)}(q)\epsilon_\nu^{(\lambda)*}(q) = -g_{\mu\nu} + \frac{q_\mu q_\nu}{m_W^2}. \tag{4.54}$$

Summing over final spins and averaging over the three initial polarisations gives

$$\overline{|\mathcal{M}|^2} = \frac{g^2m_W^2}{3}. \tag{4.55}$$

Equation (4.49) therefore gives

$$\Gamma(W \to \ell\nu) = \frac{g^2m_W}{48\pi}. \tag{4.56}$$

Finally, using Eq. (4.50),

$$\boxed{\Gamma(W \to \ell\nu) = \frac{G_Fm_W^3}{6\pi\sqrt{2}}.} \tag{4.57}$$

This is a partial width: it describes one specified decay channel rather than all possible W decays. Lepton universality predicts the same result for e, μ and τ, apart from small mass effects and radiative corrections.

For a quark channel,

$$\Gamma(W \to u_i\bar{d}_j) = N_c|V_{ij}|^2\frac{G_Fm_W^3}{6\pi\sqrt{2}}\left[1 + \delta_{\text{QCD}} + \cdots\right], \tag{4.58}$$

where u_i and d_j are up- and down-type quarks, $N_c = 3$ counts colour, and V_{ij} is the relevant element of the CKM matrix. The leading strong- interaction correction is $\delta_{\text{QCD}} \simeq \alpha_s(m_W)/\pi$; the ellipsis denotes higher-order QCD and electroweak corrections and quark-mass effects. Summing over all kinematically allowed channels tests both colour counting and CKM unitarity. The top quark is too heavy to occur in an on-shell W decay.

4.3.3 Z partial widths

For $Z(q) \to f(p_1)\bar{f}(p_2)$, the interaction convention used here gives

$$\mathcal{M} = -\frac{g}{2c_W}\bar{u}_f(p_1)\gamma^\mu(g_V^f - g_A^f\gamma^5)v_f(p_2)\epsilon_\mu(q). \tag{4.59}$$

Recall that $c_W = \cos\theta_W$, $g_V^f = T_3^f - 2Q_f s_W^2$ and $g_A^f = T_3^f$. The colour factor is $N_c^f = 1$ for leptons and $N_c^f = 3$ for quarks. For $m_f \ll m_Z$, the spin and polarisation sums give

$$\overline{|\mathcal{M}|^2} = N_c^f \frac{g^2 m_Z^2}{3c_W^2}\left[(g_V^f)^2 + (g_A^f)^2\right]. \tag{4.60}$$

Consequently,

$$\Gamma(Z \to f\bar{f}) = N_c^f \frac{g^2 m_Z}{48\pi c_W^2}\left[(g_V^f)^2 + (g_A^f)^2\right]. \tag{4.61}$$

Using $m_W = m_Z c_W$ in Eq. (4.50) gives

$$\frac{g^2}{c_W^2} = 4\sqrt{2}\,G_F m_Z^2, \tag{4.62}$$

and hence

$$\boxed{\Gamma(Z \to f\bar{f}) = N_c^f \frac{G_F m_Z^3}{6\pi\sqrt{2}}\left[(g_V^f)^2 + (g_A^f)^2\right].} \tag{4.63}$$

For quarks this expression receives sizeable QCD corrections. Precision predictions also include electroweak corrections, final-state photon radiation, fermion masses and appropriately defined effective couplings.

The total width is the sum over all kinematically accessible partial widths,

$$\Gamma_Z = \sum_f \Gamma_f, \qquad \mathrm{BR}(Z \to f\bar{f}) = \frac{\Gamma_f}{\Gamma_Z}. \tag{4.64}$$

Here $\Gamma_f \equiv \Gamma(Z \to f\bar{f})$, while the branching fraction is the fraction of all Z decays producing that final state. The lifetime is related to the total width by $\tau_Z = \hbar/\Gamma_Z$, or $\tau_Z = 1/\Gamma_Z$ in natural units.

Invisible decays are dominated by $Z \to \nu\bar{\nu}$. Since the coupling of one light active neutrino species is predicted, the invisible width determines

$$N_\nu = \frac{\Gamma_{\mathrm{inv}}}{\Gamma(Z \to \nu\bar{\nu})_{\text{one species}}}. \tag{4.65}$$

Only species lighter than $m_Z/2$ contribute to this on-shell two-body decay. The line-shape measurement therefore established that there are three light active neutrinos with the Standard Model Z coupling. It does not exclude heavier neutrinos or sterile states that do not couple to the Z in this way.

Experimental connection

A partial width is not measured by watching an isolated boson decay. It is inferred from event counts, efficiencies, luminosity, backgrounds and the shape of the resonance. Ratios such as $R_\ell = \Gamma_{\mathrm{had}}/\Gamma_\ell$ cancel important common systematics and are often more precise than absolute rates.

4.4 Resonances and the Z line shape

An unstable particle appears through a pole shifted away from the real axis. Near the Z resonance, the propagator denominator is schematically

$$\frac{1}{s - m_Z^2 + i m_Z \Gamma_Z}. \tag{4.66}$$

The corresponding Breit–Wigner structure is

$$\sigma_f(s) \propto \frac{\Gamma_e \Gamma_f}{(s - m_Z^2)^2 + m_Z^2 \Gamma_Z^2}. \tag{4.67}$$

At the pole, after adopting the standard line-shape convention, the peak cross section is

$$\sigma_f^0 = \frac{12\pi}{m_Z^2} \frac{\Gamma_e \Gamma_f}{\Gamma_Z^2}. \tag{4.68}$$

Scanning the centre-of-mass energy across the resonance separately determines the location of the peak, its width and channel-dependent normalisations.

Real data require more than the elementary Breit–Wigner expression. Initial- state radiation lowers the effective collision energy and distorts the line shape; photon exchange and γ–Z interference contribute away from the exact pole; beam-energy calibration and beam-energy spread matter directly. The experimentally quoted pseudo-observables are obtained after unfolding these effects within a specified framework.

Key idea

Precision observables are never just raw event counts. They are carefully defined quantities obtained by correcting for radiation, detector response and known backgrounds. Theory and experiment must use the same definition before their numbers can be meaningfully compared.

4.5 Angular distributions and parity-violating asymmetries

Consider $e^+e^- \to Z \to f\bar{f}$ near the Z pole, with unpolarised beams and negligible fermion masses. The angular dependence may be written as

$$\frac{\mathrm{d}\sigma}{\mathrm{d}\cos\theta} \propto (1 + \cos^2\theta) + 2A_e A_f \cos\theta, \tag{4.69}$$

where θ is the angle between the incoming electron and outgoing fermion, and

$$A_f = \frac{2 g_V^f g_A^f}{(g_V^f)^2 + (g_A^f)^2} = \frac{(g_L^f)^2 - (g_R^f)^2}{(g_L^f)^2 + (g_R^f)^2}. \tag{4.70}$$

The symmetric term determines the total rate. The term odd in $\cos\theta$ is an interference effect and produces a forward–backward asymmetry,

$$A_{\mathrm{FB}}^f \equiv \frac{\sigma_F - \sigma_B}{\sigma_F + \sigma_B} = \frac{3}{4} A_e A_f \tag{4.71}$$

at the pole. With a longitudinally polarised electron beam, the left–right asymmetry is

$$A_{\mathrm{LR}} = \frac{\sigma_L - \sigma_R}{\sigma_L + \sigma_R} = A_e. \tag{4.72}$$

Polarisation therefore isolates the electron coupling without requiring the coupling of a chosen final state.

For charged leptons, $g_V^\ell = -1/2 + 2s_W^2$ is accidentally small because s_W^2 is close to 1/4. Consequently A_ℓ is highly sensitive to small changes in the effective weak mixing angle. This is an excellent example of observable design: an asymmetry can be much more sensitive to a parameter than an inclusive rate even when it uses fewer events.

At hadron colliders the quark direction is not known event by event. In a proton–proton collision it is inferred statistically from the boost of the dilepton system, since a valence quark typically carries more momentum than a sea antiquark. Angular coefficients in Drell–Yan events then provide access to $\sin^2\theta_W$ and to the chiral quark couplings, with parton-distribution uncertainties forming an important part of the analysis.

4.6 Charged-current production and the special problem of m_W

At a hadron collider the dominant subprocesses include

$$u\bar{d} \to W^+ \to \ell^+\nu, \qquad d\bar{u} \to W^- \to \ell^-\bar{\nu}. \tag{4.73}$$

The neutrino is not detected, and the unknown longitudinal momenta of the initial partons prevent complete reconstruction of the invariant mass. Instead one uses transverse quantities. The transverse mass is

$$m_T^2 = 2p_T^\ell p_T^{\text{miss}}\left(1 - \cos\Delta\phi_{\ell,\text{miss}}\right). \tag{4.74}$$

For an ideal on-shell two-body decay with perfect resolution, $m_T \le m_W$, producing a Jacobian edge near the mass. The charged-lepton p_T spectrum and missing transverse momentum contain complementary information.

Extracting m_W at high precision requires excellent calibration of lepton momenta and hadronic recoil, as well as accurate modelling of QED radiation, the W transverse-momentum distribution and proton parton distributions. This is why a mass that appears as a simple parameter in the Lagrangian becomes a complex global experimental analysis.

The W charge asymmetry,

$$A_W(y) = \frac{\mathrm{d}\sigma(W^+)/\mathrm{d}y - \mathrm{d}\sigma(W^-)/\mathrm{d}y}{\mathrm{d}\sigma(W^+)/\mathrm{d}y + \mathrm{d}\sigma(W^-)/\mathrm{d}y}, \tag{4.75}$$

is sensitive to the proton's u and d distributions. Electroweak measurements and QCD structure are therefore entangled: improved parton distributions sharpen electroweak tests, while W/Z data themselves constrain the parton distributions.

4.7 Low-energy neutral-current checks

When $|q^2| \ll m_Z^2$, Z exchange again looks like a four-fermion interaction. Neutrino scattering, parity-violating electron scattering and atomic parity violation therefore test the same neutral-current couplings as Z-pole experiments, but at very different momentum transfers. Their main conceptual role is to test the predicted running of the weak mixing angle and to search indirectly for new contact interactions.

4.8 Choosing electroweak input parameters

At tree level the electroweak sector may be described using g, g' and v. Experiments instead determine physical quantities. A common input set is

$$\{\alpha,\, G_F,\, m_Z\}. \tag{4.76}$$

At tree level,

$$e^2 = 4\pi\alpha, \qquad v^2 = \frac{1}{\sqrt{2}G_F}, \qquad m_Z^2 = \frac{v^2}{4}(g^2 + g'^2). \tag{4.77}$$

Combining these equations yields

$$s_W^2 c_W^2 = \frac{\pi\alpha}{\sqrt{2}G_F m_Z^2}, \tag{4.78}$$

and then $m_W^2 = m_Z^2 c_W^2$. Thus three precisely measured inputs predict a fourth observable.

Beyond tree level, parameters such as α and s_W^2 depend on the renormalisation prescription and scale. Common schemes include the on-shell definition

$$s_W^2 \equiv 1 - \frac{m_W^2}{m_Z^2} \tag{4.79}$$

and running $\overline{\text{MS}}$ quantities. These are not competing physical truths. They are different book-keeping conventions; any complete prediction for a measurable quantity agrees up to terms beyond the calculated order.

Checkpoint

A bare or renormalised Lagrangian parameter is not automatically an observable. Whenever quoting $\sin^2\theta_W$, specify the definition and scale. The effective weak mixing angle extracted from asymmetries is not numerically identical to the on-shell quantity $1 - m_W^2/m_Z^2$.

4.9 Radiative corrections: sensitivity to virtual heavy particles

Loop corrections modify the tree-level relation among G_F, α, m_Z and m_W. In the on-shell scheme they are conventionally collected into Δr:

$$m_W^2\left(1 - \frac{m_W^2}{m_Z^2}\right) = \frac{\pi\alpha}{\sqrt{2}G_F}\frac{1}{1-\Delta r}. \tag{4.80}$$

The precise organisation of higher-order terms depends on convention, but the physical content is clear. Vacuum polarisation makes the electromagnetic coupling run; weak-isospin breaking affects the relation between neutral and charged currents; vertex and box corrections modify muon decay and other processes.

An especially important contribution is the top–bottom mass splitting. At one loop, the leading heavy-top correction to the rho parameter is

$$\Delta\rho \simeq \frac{3G_F m_t^2}{8\pi^2\sqrt{2}}. \tag{4.81}$$

The quadratic dependence on m_t reflects strong breaking of weak isospin within the $(t, b)_L$ doublet. Historically, precision electroweak data were sensitive to the top mass before the top quark was directly observed. Higgs contributions to many precision observables are only logarithmically sensitive to m_h at leading order, but global fits also provided indirect information about the Higgs mass before its discovery.

This illustrates non-decoupling. Heavy particles do not always disappear from low-energy observables if their masses originate from symmetry breaking or if they strongly violate a symmetry. Decoupling must be established from the structure of the theory rather than assumed from mass alone.

4.10 Interpreting a deviation

A discrepancy should not immediately be assigned to one vertex. Gauge symmetry correlates masses and couplings, and experimental and theoretical uncertainties are shared between measurements. New physics that mainly modifies gauge-boson propagators is often summarised by the oblique parameters S and T; more general heavy new physics can be described using Standard Model effective field theory. For this course, the essential point is that any interpretation must use a consistent set of observables, input parameters and correlations. High-energy tails may enhance new-physics effects, but they must remain below the scale where the effective description breaks down.

4.11 Summary

The electroweak Lagrangian predicts not only the existence of W and Z bosons but a network of rates and asymmetries. For massless fermions,

$$\Gamma(W \to \ell\nu) = \frac{G_F m_W^3}{6\pi\sqrt{2}}, \tag{4.82}$$

and

$$\Gamma(Z \to f\bar{f}) = N_c^f \frac{G_F m_Z^3}{6\pi\sqrt{2}} \left[(g_V^f)^2 + (g_A^f)^2\right]. \tag{4.83}$$

The Z line shape determines masses, widths and branching fractions, while angular and polarisation asymmetries isolate chiral couplings. Low-energy neutral-current measurements test the same theory far below the weak scale.

At tree level, $\{\alpha, G_F, m_Z\}$ predicts m_W. Loop corrections introduce sensitivity to the top mass, Higgs sector and possible new particles. Oblique parameters and SMEFT provide increasingly general languages for organising deviations, provided their assumptions and validity domains are respected.

Checkpoint

Three lessons should survive beyond the formulae:

1. Total rates measure mostly coupling magnitudes; asymmetries expose chirality and interference.
2. Precision comparison requires a common definition, input scheme and radiative-correction framework.
3. Electroweak observables form a correlated system: a genuine new-physics effect should generally appear consistently in more than one place.

Short exercises

1. Calculate g_V and g_A for ν, e, u, d. Why are charged-lepton asymmetries especially sensitive to s_W^2?
2. Integrate the pole angular distribution and derive $A_{\rm FB}^f = 3A_eA_f/4$.
3. Derive Eq. (4.78) from $e = gs_W$, $m_W = gv/2$, $m_Z = m_W/c_W$ and $G_F = 1/(\sqrt{2}v^2)$.
4. Why is transverse mass used in $W \to \ell\nu$ measurements rather than an ordinary reconstructed invariant mass?

Chapter 5

Flavour Physics, CP Violation and the Muon Anomalous Moment

Flavour physics searches for new particles without necessarily producing them: quantum amplitudes allow heavy virtual states to alter rare transitions, oscillations and precision magnetic moments.

The gauge sector of the Standard Model is highly constrained, but the flavour sector is not. Gauge symmetry tells us how quarks and leptons interact once their quantum numbers are known; it does not explain why there are three generations, why their masses span many orders of magnitude, or why their mixing angles have the observed pattern. These unexplained parameters reside in the Yukawa matrices.

In this lecture we first derive the *Cabibbo–Kobayashi–Maskawa* (CKM) matrix and explain the history encoded in its name. We then study unitarity, charge–parity (CP) violation, neutral-meson mixing and the *Glashow–Iliopoulos–Maiani* (GIM) mechanism. The final part introduces the muon anomalous magnetic moment, usually called muon $g-2$. Although $g-2$ is flavour conserving, it uses the same precision-frontier strategy: small loop effects can reveal virtual physics at scales much higher than the muon mass.

The three generations of quarks and leptons

The Standard Model contains three generations, or families, of quarks and leptons. Each generation has the same gauge quantum numbers but different fermion masses. The generation label is therefore a flavour label rather than a different type of gauge charge.

The corresponding left-handed weak doublets are

$$Q_L^1 = \begin{pmatrix} u_L \\ d_L \end{pmatrix}, \qquad Q_L^2 = \begin{pmatrix} c_L \\ s_L \end{pmatrix}, \qquad Q_L^3 = \begin{pmatrix} t_L \\ b_L \end{pmatrix}, \tag{5.1}$$

and

$$L_L^1 = \begin{pmatrix} \nu_{eL} \\ e_L \end{pmatrix}, \qquad L_L^2 = \begin{pmatrix} \nu_{\mu L} \\ \mu_L \end{pmatrix}, \qquad L_L^3 = \begin{pmatrix} \nu_{\tau L} \\ \tau_L \end{pmatrix}. \tag{5.2}$$

Here Q_L^i denotes a left-handed quark doublet, L_L^i denotes a left-handed lepton doublet, and $i = 1, 2, 3$ is the generation index. Within each doublet, the upper field has weak isospin $T_3 = +1/2$, while the lower field has $T_3 = -1/2$.

Table 5.1: The three generations of Standard Model fermions.

Particle type	Generation 1	Generation 2	Generation 3	Charge
Up-type quark	u up	c charm	t top	$+\frac{2}{3}$
Down-type quark	d down	s strange	b bottom	$-\frac{1}{3}$
Charged lepton	e^- electron	μ^- muon	τ^- tau	-1
Neutrino	ν_e electron neutrino	ν_μ muon neutrino	ν_τ tau neutrino	0

The corresponding right-handed charged fermions,

$$u_R,\ c_R,\ t_R, \qquad d_R,\ s_R,\ b_R, \qquad e_R,\ \mu_R,\ \tau_R, \tag{5.3}$$

are $SU(2)_L$ singlets. In the minimal Standard Model there are no right-handed neutrino fields.

Key idea

The three generations have identical electroweak quantum numbers but different masses. Quark flavour mixing arises because the weak-interaction states and mass eigenstates are not aligned. The corresponding mixing matrix for quarks is the CKM matrix; in the lepton sector, neutrino mixing is described by the Pontecorvo–Maki–Nakagawa–Sakata (PMNS) matrix.

5.1 Flavour begins with the Yukawa matrices

For three generations, the quark Yukawa interactions are

$$\mathcal{L}_Y^q = -\bar{Q}_L^i (Y_d)_{ij} \Phi d_R^j - \bar{Q}_L^i (Y_u)_{ij} \widetilde{\Phi} u_R^j + \text{h.c.}, \tag{5.4}$$

where $i, j = 1, 2, 3$ are generation indices and repeated indices are summed. The field $Q_L^i = (u_L^i, d_L^i)^T$ is a left-handed quark weak doublet; u_R^j and d_R^j are right-handed weak singlets; Y_u and Y_d are complex 3×3 Yukawa-coupling matrices; and $\widetilde{\Phi} = i\sigma^2 \Phi^*$ is the conjugate Higgs doublet. The notation "h.c." means Hermitian conjugate. After $\langle \Phi \rangle = (0, v/\sqrt{2})^T$, where $v \simeq 246$ GeV is the Higgs vacuum expectation value, the Yukawa interactions generate

$$M_u = \frac{v}{\sqrt{2}} Y_u, \qquad M_d = \frac{v}{\sqrt{2}} Y_d. \tag{5.5}$$

These matrices need not be diagonal in the weak-interaction basis. The weak basis is the basis in which the gauge interactions have their simplest form; the mass basis is the basis in which the propagating quarks have definite masses.

Any complex matrix admits a singular-value decomposition. We therefore choose unitary matrices satisfying

$$U_{uL}^\dagger M_u U_{uR} = \text{diag}(m_u, m_c, m_t), \qquad U_{dL}^\dagger M_d U_{dR} = \text{diag}(m_d, m_s, m_b). \tag{5.6}$$

The mass eigenstates are related to the weak eigenstates by, for example, $u_L^{\text{weak}} = U_{uL} u_L^{\text{mass}}$. Right-handed rotations do not enter the charged weak current because u_R and d_R are $SU(2)_L$ singlets.

In the weak basis the charged current is

$$\mathcal{L}_{\mathrm{cc}}^{q} = -\frac{g}{\sqrt{2}}\bar{u}_L^{\mathrm{weak}}\gamma^\mu d_L^{\mathrm{weak}} W_\mu^+ + \mathrm{h.c.} \tag{5.7}$$

Transforming both fields to their mass bases produces

$$\mathcal{L}_{\mathrm{cc}}^{q} = -\frac{g}{\sqrt{2}}\bar{u}_L\gamma^\mu V_{\mathrm{CKM}} d_L W_\mu^+ + \mathrm{h.c.}, \qquad \boxed{V_{\mathrm{CKM}} = U_{uL}^\dagger U_{dL}.} \tag{5.8}$$

Mixing is therefore a mismatch between two basis choices. There is no absolute meaning to the rotation of the up or down sector separately; only their relative rotation is observable.

Neutral currents have the form $\bar{d}_L^{\mathrm{weak}}\gamma^\mu d_L^{\mathrm{weak}}$. After rotation they contain $U_{dL}^\dagger U_{dL} = \mathbf{1}$ and remain flavour diagonal. The same is true of the photon, Z and Higgs couplings at tree level in the minimal Standard Model. This is the first reason flavour-changing neutral currents are rare.

Key idea

The CKM matrix is not an additional interaction inserted by hand. It appears because the two quarks in a weak doublet cannot, in general, both be placed in their mass bases by the same left-handed rotation.

5.2 Why is it called the CKM matrix?

The name records three stages in the history of quark mixing. In 1963, Nicola Cabibbo described mixing between the first two quark generations using one angle, now called the Cabibbo angle. In 1970, Sheldon Glashow, John Iliopoulos and Luciano Maiani showed that adding the charm quark produces cancellations that suppress unwanted neutral-current flavour change. In 1973, Makoto Kobayashi and Toshihide Maskawa showed that a three-generation quark-mixing matrix contains an irreducible complex phase capable of producing CP violation. Their argument implied the need for a third generation before the bottom and top quarks were discovered. The modern three-generation matrix is therefore called the Cabibbo–Kobayashi–Maskawa matrix.

5.3 The structure and parameters of the CKM matrix

Writing $u = (u, c, t)^T$ and $d = (d, s, b)^T$,

$$V_{\mathrm{CKM}} = \begin{pmatrix} V_{ud} & V_{us} & V_{ub} \\ V_{cd} & V_{cs} & V_{cb} \\ V_{td} & V_{ts} & V_{tb} \end{pmatrix}. \tag{5.9}$$

Here u, c, t denote the up, charm and top quarks, while d, s, b denote the down, strange and bottom quarks. The element V_{ij} is the relative charged-current amplitude for an up-type quark i to couple to a down-type quark j; a decay rate normally contains $|V_{ij}|^2$. It is unitary because it is a product of unitary matrices:

$$V^\dagger V = VV^\dagger = \mathbf{1}. \tag{5.10}$$

A general 3×3 unitary matrix contains nine real parameters. Five phases can be removed by rephasing the six quark fields; one common phase leaves every bilinear unchanged and cannot be used independently. Four physical parameters remain: three mixing angles and one irreducible CP-violating phase.

The standard parametrisation is

$$V = \begin{pmatrix} c_{12}c_{13} & s_{12}c_{13} & s_{13}e^{-i\delta} \\ -s_{12}c_{23} - c_{12}s_{23}s_{13}e^{i\delta} & c_{12}c_{23} - s_{12}s_{23}s_{13}e^{i\delta} & s_{23}c_{13} \\ s_{12}s_{23} - c_{12}c_{23}s_{13}e^{i\delta} & -c_{12}s_{23} - s_{12}c_{23}s_{13}e^{i\delta} & c_{23}c_{13} \end{pmatrix}, \tag{5.11}$$

where $s_{ij} \equiv \sin\theta_{ij}$, $c_{ij} \equiv \cos\theta_{ij}$ and δ is the physical CP-violating phase. The hierarchy is more visible in the Wolfenstein expansion,

$$V \simeq \begin{pmatrix} 1-\lambda^2/2 & \lambda & A\lambda^3(\rho - i\eta) \\ -\lambda & 1-\lambda^2/2 & A\lambda^2 \\ A\lambda^3(1-\rho-i\eta) & -A\lambda^2 & 1 \end{pmatrix} + \mathcal{O}(\lambda^4), \tag{5.12}$$

where $\lambda \simeq 0.225$ is approximately $|V_{us}|$, A sets the size of second–third-generation mixing, and ρ and η encode the magnitude and complex phase of first–third-generation mixing. The notation $\mathcal{O}(\lambda^4)$ denotes fourth- and higher-order terms. Transitions within neighbouring generations are suppressed by powers of λ, and transitions between the first and third generations are particularly small.

For N generations a unitary mixing matrix contains

$$\frac{N(N-1)}{2} \text{ angles}, \qquad \frac{(N-1)(N-2)}{2} \text{ physical phases}. \tag{5.13}$$

With two generations there is one Cabibbo angle but no physical CP phase. At least three generations are required for CKM CP violation.

5.4 Unitarity triangles

Off-diagonal entries of Eq. (5.10) give six orthogonality relations. The one most useful for B physics is

$$V_{ud}V_{ub}^* + V_{cd}V_{cb}^* + V_{td}V_{tb}^* = 0. \tag{5.14}$$

5.4.1 Constructing the unitarity triangle

The unitarity of the Cabibbo–Kobayashi–Maskawa matrix implies

$$V_{\mathrm{CKM}}^\dagger V_{\mathrm{CKM}} = V_{\mathrm{CKM}} V_{\mathrm{CKM}}^\dagger = \mathbf{1}. \tag{5.15}$$

The orthogonality of the first and third columns gives

$$V_{ud}V_{ub}^* + V_{cd}V_{cb}^* + V_{td}V_{tb}^* = 0. \tag{5.16}$$

Each term is a complex number. Equation (5.16) therefore states that three vectors in the complex plane add to zero and form a closed triangle.

To obtain the conventional normalised triangle, divide Eq. (5.16) by $-V_{cd}V_{cb}^*$:

$$-\frac{V_{ud}V_{ub}^*}{V_{cd}V_{cb}^*} - \frac{V_{td}V_{tb}^*}{V_{cd}V_{cb}^*} = 1. \tag{5.17}$$

The position of the apex is defined by

$$\boxed{\bar\rho + i\bar\eta \equiv -\frac{V_{ud}V_{ub}^*}{V_{cd}V_{cb}^*}}. \tag{5.18}$$

Here $\bar\rho$ and $\bar\eta$ are the improved Wolfenstein parameters, including higher-order corrections to the original parameters ρ and η. The three vertices of the normalised unitarity triangle are therefore

$$(0,0), \qquad (1,0), \qquad (\bar\rho, \bar\eta). \tag{5.19}$$

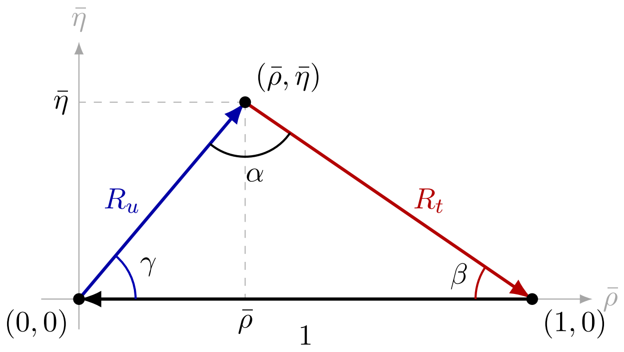

5.4.2 How CKM unitarity provides precision tests

The Standard Model requires the CKM matrix to be exactly unitary. This produces two complementary kinds of precision test:

1. the normalisation of each row and column must equal one;
2. different complex products of CKM elements must form closed unitarity triangles.

Row and column normalisation

The first-row condition is

$$\boxed{|V_{ud}|^2 + |V_{us}|^2 + |V_{ub}|^2 = 1.} \tag{5.20}$$

The three terms can be determined from different processes:

$$\begin{aligned} |V_{ud}| &: \quad \text{superallowed nuclear beta decays and neutron decay,} \\ |V_{us}| &: \quad \text{kaon and tau decays,} \\ |V_{ub}| &: \quad \text{semileptonic bottom-hadron decays.} \end{aligned} \tag{5.21}$$

A useful measure of possible non-unitarity is

$$\Delta^{(1)}_{\text{CKM}} \equiv |V_{ud}|^2 + |V_{us}|^2 + |V_{ub}|^2 - 1. \tag{5.22}$$

The Standard Model predicts

$$\boxed{\Delta^{(1)}_{\text{CKM}} = 0.} \tag{5.23}$$

A statistically significant nonzero value could indicate an experimental or theoretical problem, or new physics such as mixing with additional quarks, modified charged currents or non-standard beta-decay interactions.

Similarly, the third-column condition is

$$|V_{ub}|^2 + |V_{cb}|^2 + |V_{tb}|^2 = 1. \tag{5.24}$$

Since $|V_{tb}|$ is close to unity, this relation is tested through top-quark production and decay together with flavour measurements of $|V_{ub}|$ and $|V_{cb}|$.

More generally, CKM unitarity can be written as

$$\boxed{\sum_{i=u,c,t} V_{ij} V^*_{ik} = \delta_{jk},} \tag{5.25}$$

where δ_{jk} is the Kronecker delta:

$$\delta_{jk} = \begin{cases} 1, & j = k, \\ 0, & j \neq k. \end{cases} \tag{5.26}$$

For $j = k$, Eq. (5.25) gives column normalisation. For $j \neq k$, it gives an orthogonality relation and hence a unitarity triangle.

Triangle closure

For the bottom–down triangle,

$$V_{ud}V_{ub}^* + V_{cd}V_{cb}^* + V_{td}V_{tb}^* = 0. \tag{5.27}$$

A convenient closure parameter is

$$\Delta_{bd} \equiv V_{ud}V_{ub}^* + V_{cd}V_{cb}^* + V_{td}V_{tb}^*. \tag{5.28}$$

The Standard Model predicts

$$\boxed{\Delta_{bd} = 0.} \tag{5.29}$$

This is a complex equation, so it represents two independent tests:

$$\Re(\Delta_{bd}) = 0, \qquad \Im(\Delta_{bd}) = 0. \tag{5.30}$$

Equivalently, the independently measured sides and angles must satisfy

$$\alpha + \beta + \gamma = \pi \tag{5.31}$$

and must identify one common apex $(\bar{\rho}, \bar{\eta})$.

Tree-level and loop-level constraints

Different observables constrain different parts of the triangle:

$$R_u = \left| \frac{V_{ud}V_{ub}^*}{V_{cd}V_{cb}^*} \right|, \qquad \text{from tree-level semileptonic decays,} \tag{5.32}$$

$$\gamma = \arg\left[-\frac{V_{ud}V_{ub}^*}{V_{cd}V_{cb}^*} \right], \qquad \text{from tree-dominated } B \to DK \text{ decays,} \tag{5.33}$$

$$\sin(2\beta) \simeq S_{J/\psi K_S}, \qquad \text{from time-dependent CP violation in } B^0 \to J/\psi K_S, \tag{5.34}$$

$$\frac{\Delta m_d}{\Delta m_s} \propto \left| \frac{V_{td}}{V_{ts}} \right|^2 \frac{f_{B_d}^2 B_{B_d}}{f_{B_s}^2 B_{B_s}}, \qquad \text{from } B_d^0 \text{ and } B_s^0 \text{ mixing.} \tag{5.35}$$

Here:

- Δm_d and Δm_s are the mass splittings between the heavy and light neutral-B_d and neutral-B_s mass eigenstates;
- f_{B_q} is a neutral-B_q decay constant;
- B_{B_q} is a bag parameter describing the relevant hadronic matrix element;
- $S_{J/\psi K_S}$ is the coefficient of the sine term in the time-dependent CP asymmetry.

Tree-level determinations are expected to be comparatively insensitive to heavy new particles. Meson mixing and rare decays occur through loops and can receive additional virtual contributions. A particularly powerful test is therefore to determine the apex using tree-level measurements and ask whether loop-dominated measurements select the same point.

Schematically,

$$\boxed{(\bar\rho,\bar\eta)_{\text{tree}} \overset{\text{SM}}{=} (\bar\rho,\bar\eta)_{\text{loop}}.} \tag{5.36}$$

If the two regions fail to overlap after all experimental and theoretical uncertainties are included, the CKM description is incomplete or a new particle contributes to the loop amplitudes.

Experimental connection

A global CKM fit combines measurements with different dependences on CKM elements, CP phases and hadronic matrix elements. The important test is not whether one observable agrees with the Standard Model in isolation, but whether all independent constraints overlap in a common region of the $(\bar\rho,\bar\eta)$ plane.

The normalised CKM unitarity triangle. The precise apex shown is illustrative; experimentally allowed regions are obtained from a global fit to many observables.

The lengths of the two non-trivial sides are

$$R_u \equiv \left|\frac{V_{ud}V_{ub}^*}{V_{cd}V_{cb}^*}\right| = \sqrt{\bar\rho^2+\bar\eta^2}, \tag{5.37}$$

$$R_t \equiv \left|\frac{V_{td}V_{tb}^*}{V_{cd}V_{cb}^*}\right| = \sqrt{(1-\bar\rho)^2+\bar\eta^2}. \tag{5.38}$$

The base has unit length because of the normalisation chosen in Eq. (5.17).

The angles are

$$\alpha = \arg\left[-\frac{V_{td}V_{tb}^*}{V_{ud}V_{ub}^*}\right], \tag{5.39}$$

$$\beta = \arg\left[-\frac{V_{cd}V_{cb}^*}{V_{td}V_{tb}^*}\right], \tag{5.40}$$

$$\gamma = \arg\left[-\frac{V_{ud}V_{ub}^*}{V_{cd}V_{cb}^*}\right]. \tag{5.41}$$

Since these are the three internal angles of a triangle,

$$\boxed{\alpha+\beta+\gamma=\pi.} \tag{5.42}$$

A nonzero value of $\bar\eta$ gives a triangle with nonzero area and signals CP violation. If $\bar\eta=0$, the triangle collapses to a straight line and CKM CP violation vanishes.

Key idea

The unitarity triangle is not a separate model or an additional assumption. It is a geometrical representation of one orthogonality condition implied by the unitarity of the CKM matrix.

The star denotes complex conjugation. Each term is complex, so the three vectors form a closed triangle in the complex plane. Dividing by $V_{cd}V_{cb}^*$ produces the conventional normalised unitarity triangle with vertices near $(0,0)$, $(1,0)$ and $(\bar\rho,\bar\eta)$.

Its angles are conventionally defined by

$$\alpha = \arg\left[-\frac{V_{td}V_{tb}^*}{V_{ud}V_{ub}^*}\right], \tag{5.43}$$

$$\beta = \arg\left[-\frac{V_{cd}V_{cb}^*}{V_{td}V_{tb}^*}\right], \tag{5.44}$$

$$\gamma = \arg\left[-\frac{V_{ud}V_{ub}^*}{V_{cd}V_{cb}^*}\right], \tag{5.45}$$

and $\alpha+\beta+\gamma=\pi$. Different observables determine sides and angles. If all measurements meet at one apex, the CKM description is successful. New particles entering loops can shift mixing or rare-decay constraints without changing tree-level determinations, preventing closure.

The rephasing-invariant measure of CP violation is the Jarlskog invariant,

$$J = \Im(V_{ij}V_{kl}V_{il}^*V_{kj}^*) = c_{12}c_{23}c_{13}^2 s_{12}s_{23}s_{13}\sin\delta, \tag{5.46}$$

for any choice of distinct $i \neq k$ and $j \neq l$, up to a sign. Every CKM unitarity triangle has area $|J|/2$. CP violation vanishes if any relevant mixing angle vanishes, if $\delta = 0$ or π, or if two equal-charge quarks are mass degenerate so that an additional rotation removes the phase.

Checkpoint

Complex entries in a particular matrix convention are not themselves physical. A CP-odd observable must depend on a rephasing-invariant combination such as J, together with both weak-phase and strong-phase differences when a direct rate asymmetry is measured.

5.5 How CP violation appears

The combined transformation CP consists of two operations. Charge conjugation, denoted by C, replaces every particle by its antiparticle, while parity, denoted by P, reverses the spatial coordinates, $\mathbf{x} \to -\mathbf{x}$. A process violates CP symmetry if its probability differs from that of the corresponding CP-conjugate process. For example, direct CP violation occurs if

$$\Gamma(P \to f) \neq \Gamma(\overline{P} \to \overline{f}), \tag{5.47}$$

where P is a particle, $\overline{P}$ is its antiparticle, and f and $\overline{f}$ are the corresponding final states.

In the Standard Model, CP violation in quark-flavour processes originates from the irreducible complex phase in the Cabibbo–Kobayashi–Maskawa (CKM) matrix. However, a complex CKM element alone is not sufficient to produce a difference between a decay rate and its CP-conjugate rate. At least two amplitudes with different phases must interfere.

Suppose that a decay $P \to f$ receives two contributions:

$$A_f = A_1 e^{i(\delta_1+\phi_1)} + A_2 e^{i(\delta_2+\phi_2)}. \tag{5.48}$$

Here A_1 and A_2 are real, positive magnitudes. The phases have two different physical origins:

- ϕ_i are called *weak phases*. They arise from complex CKM factors and change sign under CP:

$$\phi_i \longrightarrow -\phi_i.$$

- δ_i are called *strong phases*. They arise from final-state rescattering or from absorptive parts of loop amplitudes. They do not change sign under CP:

$$\delta_i \longrightarrow \delta_i.$$

Consequently, the amplitude for the CP-conjugate process is

$$\overline{A}_{\overline{f}} = A_1 e^{i(\delta_1-\phi_1)} + A_2 e^{i(\delta_2-\phi_2)}. \tag{5.49}$$

Notice that CP conjugation reverses the weak phases but leaves the strong phases unchanged. Squaring the two amplitudes gives

$$|A_f|^2 = A_1^2 + A_2^2 + 2A_1A_2\cos[(\delta_1-\delta_2)+(\phi_1-\phi_2)]\,, \tag{5.50}$$

$$|\overline{A}_{\overline{f}}|^2 = A_1^2 + A_2^2 + 2A_1A_2\cos[(\delta_1-\delta_2)-(\phi_1-\phi_2)]\,. \tag{5.51}$$

Their difference is therefore

$$|A_f|^2 - |\overline{A}_{\overline{f}}|^2 = -4A_1A_2\sin(\delta_1-\delta_2)\sin(\phi_1-\phi_2). \tag{5.52}$$

The overall sign depends on the ordering chosen for the phase differences, but the physical conclusion does not: a non-zero direct CP asymmetry requires both

$$\delta_1-\delta_2 \neq 0 \qquad \text{and} \qquad \phi_1-\phi_2 \neq 0. \tag{5.53}$$

The weak-phase difference supplies the CP-violating effect. The strong-phase difference converts that effect into an observable difference between the two decay rates. If either phase difference vanishes, the direct CP asymmetry vanishes even if the individual amplitudes are complex.

A commonly measured quantity is the direct CP asymmetry

$$A_{\mathrm{CP}} = \frac{\Gamma(P\to f)-\Gamma(\overline{P}\to\overline{f})}{\Gamma(P\to f)+\Gamma(\overline{P}\to\overline{f})}. \tag{5.54}$$

Since decay rates are proportional to squared amplitudes, $A_{\mathrm{CP}} \neq 0$ signals direct CP violation.

Key idea

The term “strong phase” does *not* mean strong CP violation. A strong phase is a CP-conserving phase generated by QCD rescattering or an absorptive loop contribution. Strong CP violation instead refers to the possible QCD interaction

$$\mathcal{L}_\theta = \frac{\theta g_s^2}{32\pi^2} G^a_{\mu\nu}\widetilde{G}^{a\mu\nu},$$

whose extremely small coefficient constitutes the strong-CP problem. That is a separate subject from CKM CP violation.

Neutral mesons provide two further manifestations of CP violation:

1. *CP violation in mixing*, when the probability for $P^0 \to \overline{P}^0$ differs from that for $\overline{P}^0 \to P^0$;
2. *CP violation in the interference between mixing and decay*, when a meson can reach the same final state either directly or after oscillating into its antiparticle.

These effects are studied experimentally using flavour tagging and decay-time-dependent asymmetries. The full neutral-meson formalism is not required for the central CKM argument developed here.

Experimentally, CP violation has been observed in several quark-flavour systems: it is typically of order 10^{-3} in neutral-kaon processes, can reach 10^{-1}–1 in selected neutral-B-meson time-dependent asymmetries, and is of order 10^{-3} in charm decays. Direct CP asymmetries in some charged and neutral B decays can be at the percent to ten-percent level. CP violation has not yet been established in the lepton sector:

$$\boxed{\begin{array}{rcl} K^0 \text{ system} & : & \mathcal{O}(10^{-3}), \\ B^0_{d,s} \text{ systems} & : & \mathcal{O}(10^{-1})\text{–}\mathcal{O}(1) \quad \text{for selected mixing-induced asymmetries}, \\ D^0 \text{ and charm decays} & : & \mathcal{O}(10^{-3}), \\ \text{leptons and neutrinos} & : & \text{no conclusive observation so far.} \end{array}} \tag{5.55}$$

These numbers describe the approximate sizes of measured asymmetries, not orders in perturbation theory. Direct CP violation arises from interference between decay amplitudes and may involve tree and loop, or "penguin," contributions. Neutral-meson mixing is generated by loop-level box diagrams, while mixing-induced CP violation results from interference between direct decay and decay following oscillation.

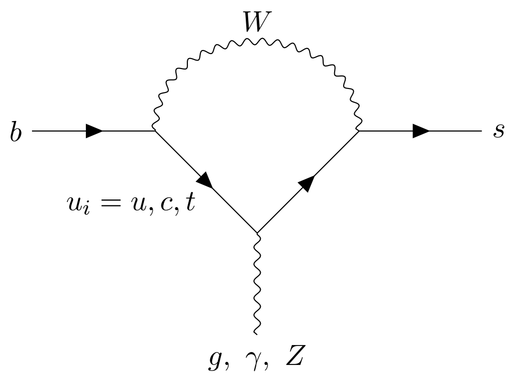

Figure 5.1: A flavour-changing $b \to s$ penguin diagram. The internal up-type quark is $u_i = u, c, t$, and the emitted neutral gauge boson may be a gluon, photon or Z boson.

For example, CP violation was first observed through $K_L \to \pi\pi$ decays; large mixing-induced asymmetries are measured in $B^0 \to J/\psi K_S$; direct CP violation occurs in several charmless B decays; and much smaller direct CP violation has been established in charm decays such as $D^0 \to K^+K^-$ and $D^0 \to \pi^+\pi^-$.

5.6 The GIM mechanism and rare neutral currents

GIM stands for the *Glashow–Iliopoulos–Maiani* mechanism, after Sheldon Glashow, John Iliopoulos and Luciano Maiani. Their 1970 construction introduced the charm quark as the weak partner needed to cancel otherwise excessive strangeness-changing neutral-current amplitudes. A flavour-changing neutral current (FCNC) changes quark flavour but carries no electric charge; examples include $s \to d$, $b \to s$ and $c \to u$. Such transitions do not occur at tree level in the Standard Model. At loop level a typical amplitude contains

$$\mathcal{M}_{d_j \to d_k} \propto \sum_{i=u,c,t} V_{ij} V_{ik}^* F\left(\frac{m_i^2}{m_W^2}\right). \tag{5.56}$$

For $j \neq k$, CKM unitarity gives

$$\sum_i V_{ij} V_{ik}^* = 0. \tag{5.57}$$

Any mass-independent part of the loop function cancels. Equivalently, one may write

$$\mathcal{M}_{d_j \to d_k} \propto \sum_i V_{ij} V_{ik}^* \left[F\left(\frac{m_i^2}{m_W^2}\right) - F(0) \right]. \tag{5.58}$$

If the internal quarks were mass-degenerate, the entire amplitude would vanish. This CKM-unitarity cancellation is the GIM mechanism.

The surviving amplitude depends on quark-mass differences. Heavy-top effects can therefore dominate K and B observables despite small CKM elements. Rare processes are unusually sensitive to new physics because the Standard Model background is suppressed by a loop factor, CKM factors, the GIM cancellation, or helicity—sometimes by all four.

Neutral-meson mixing is a $\Delta F = 2$ process generated by box diagrams. A schematic effective Hamiltonian is

$$\mathcal{H}_{\text{eff}}^{\Delta F=2} = \frac{G_F^2 m_W^2}{16\pi^2} (\text{CKM})^2 S_0(x_i)\, C(\mu)\, Q(\mu), \tag{5.59}$$

where $\mathcal{H}_{\text{eff}}$ is the low-energy effective Hamiltonian, $x_i = m_i^2/m_W^2$, S_0 is a short-distance loop function, $C(\mu)$ is a Wilson coefficient evolved to the renormalisation scale μ, and $Q(\mu)$ is a local four-quark operator. The symbol $\Delta F = 2$ means that the net flavour quantum number changes by two. The observable also requires the hadronic matrix element $\langle \bar{P}^0 | Q | P^0 \rangle$, usually supplied by lattice quantum chromodynamics (lattice QCD). Flavour phenomenology is therefore a chain connecting weak-scale matching, renormalisation-group evolution and non-perturbative QCD.

5.7 Current experimental flavour connections

Rare $b \to s\ell^+\ell^-$ transitions and neutral-meson mixing are sensitive to heavy virtual particles because their Standard Model amplitudes are loop- and CKM-suppressed. Ratios such as

$$R_K = \frac{\Gamma(B \to K\mu^+\mu^-)}{\Gamma(B \to K e^+ e^-)} \tag{5.60}$$

are theoretically clean because many hadronic uncertainties cancel. Current R_K and R_{K^*} measurements are compatible with Standard Model lepton universality [5]; the older strong-anomaly narrative is no longer current.

Charged-current ratios

$$R(D^{(*)}) = \frac{\Gamma(B \to D^{(*)}\tau\nu)}{\Gamma(B \to D^{(*)}\ell\nu)}, \qquad \ell = e, \mu, \tag{5.61}$$

and inclusive–exclusive determinations of $|V_{cb}|$ and $|V_{ub}|$ remain interesting. None is, by itself, established new physics. Detector response, form factors, correlations and control channels are part of the inference.

5.8 Magnetic moments and the meaning of $g-2$

For a spin-1/2 particle of charge q and mass m, the magnetic moment is

$$\boldsymbol{\mu} = g \frac{q}{2m} \mathbf{S}. \tag{5.62}$$

Here $\mathbf{S}$ is the spin and g is the gyromagnetic factor. The Dirac equation predicts $g = 2$ for a point-like fermion at tree level. Quantum loops shift g slightly away from two; this is why the experiment is called "g minus 2". The most general on-shell electromagnetic vertex consistent with Lorentz invariance can be written

$$\Gamma^\mu(q) = F_1(q^2)\gamma^\mu + \frac{iF_2(q^2)}{2m}\sigma^{\mu\nu}q_\nu + \cdots . \tag{5.63}$$

where q is the photon four-momentum, $\sigma^{\mu\nu} = \frac{i}{2}[\gamma^\mu, \gamma^\nu]$, F_1 is the Dirac form factor and F_2 is the Pauli form factor. Charge normalisation gives $F_1(0) = 1$, while

$$\boxed{a_\ell \equiv \frac{g_\ell - 2}{2} = F_2(0).} \tag{5.64}$$

The ellipsis can include an electric-dipole form factor, which violates CP.

Schwinger's one-loop QED result is

$$a_\ell^{\mathrm{QED}} = \frac{\alpha}{2\pi} + \mathcal{O}(\alpha^2). \tag{5.65}$$

Higher QED orders are known with extraordinary precision. Here $\alpha = e^2/(4\pi)$ is the fine-structure constant. A generic heavy particle of mass Λ gives a contribution of order

$$\Delta a_\ell \sim \frac{C}{16\pi^2}\frac{m_\ell^2}{\Lambda^2}, \tag{5.66}$$

unless an additional chirality enhancement is present. The coefficient C collects couplings and numerical factors, $1/(16\pi^2)$ is the characteristic one-loop suppression, Λ is the heavy mass scale and the factor m_ℓ^2 reflects the required chirality flip. This scaling makes the muon roughly $(m_\mu/m_e)^2 \simeq 4.3 \times 10^4$ times more sensitive than the electron to flavour-universal heavy physics, despite the electron measurement being intrinsically more precise.

5.9 How a_μ is measured

Polarised muons circulate in a magnetic storage ring. The anomalous spin-precession frequency ω_a is the difference between the spin- precession and cyclotron frequencies. At the "magic momentum" the leading electric-field contribution cancels, leaving ω_a primarily proportional to $a_\mu B$, where B is the magnetic field. Parity violation in muon decay makes the detected positron rate oscillate with the spin direction:

$$N(t) = N_0 e^{-t/(\gamma\tau_\mu)}[1 + A\cos(\omega_a t + \phi)]. \tag{5.67}$$

Here N_0 is a normalisation, τ_μ is the rest-frame muon lifetime, γ is the relativistic Lorentz factor, A is the decay asymmetry and ϕ is an initial phase. Extracting a_μ requires both ω_a and a precise magnetic-field map. Beam motion, pile-up, detector gain and lost muons are important experimental corrections.

The final Fermilab result is [7]

$$a_\mu^{\mathrm{FNAL}} = 116\,592\,070.5(14.8) \times 10^{-11}, \tag{5.68}$$

with a relative precision of 127 parts per billion (ppb). Combining it with the earlier Brookhaven measurement gives the experimental world average

$$\boxed{a_\mu^{\mathrm{exp}} = 116\,592\,071.5(14.5) \times 10^{-11}}, \tag{5.69}$$

corresponding to approximately 124 ppb precision. The notation $x(y)$ means $x \pm y$ in the final quoted digits.

5.10 The Standard Model prediction for a_μ

The prediction is organised as

$$\boxed{a_\mu^{\mathrm{SM}} = a_\mu^{\mathrm{QED}} + a_\mu^{\mathrm{EW}} + a_\mu^{\mathrm{HVP}} + a_\mu^{\mathrm{HLbL}}.} \tag{5.70}$$

The superscripts denote quantum electrodynamics (QED), electroweak interactions (EW), hadronic vacuum polarisation (HVP) and hadronic light-by-light scattering (HLbL). The following diagrams are representative rather than an exhaustive list of all perturbative orders.

5.10.1 QED: photon and charged-lepton loops

The leading correction is Schwinger's one-loop QED vertex diagram:

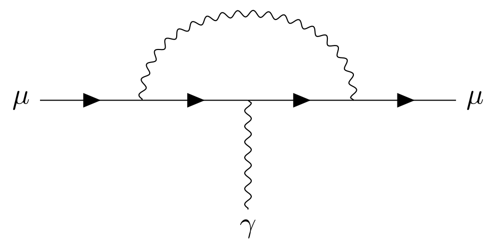

Leading QED vertex correction.

The QED result is a perturbative series in α/π. Its coefficients include electron-, muon- and tau-loop mass dependence and are known through fifth order in α. The one-loop term is analytic; the highest multiloop coefficients require large algebraic reductions and numerical integrations. QED supplies almost all of the central value of a_μ, but a negligible part of its theoretical uncertainty.

5.10.2 Electroweak loops

Electroweak diagrams contain at least one W, Z or Higgs boson. A representative W–neutrino loop is

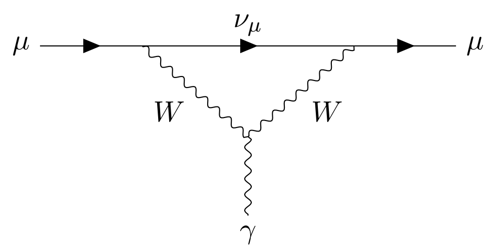

Representative one-loop electroweak contribution.

The full electroweak contribution is known at complete two-loop order, with dominant higher-order logarithms estimated using renormalisation-group methods. Its natural scale is $G_F m_\mu^2/(8\sqrt{2}\pi^2)$, so it is much smaller than the QED term but still resolvable experimentally. Its remaining uncertainty is negligible compared with the hadronic uncertainty.

5.10.3 Hadronic vacuum polarisation

Hadronic vacuum polarisation inserts a quark–gluon contribution into a photon propagator:

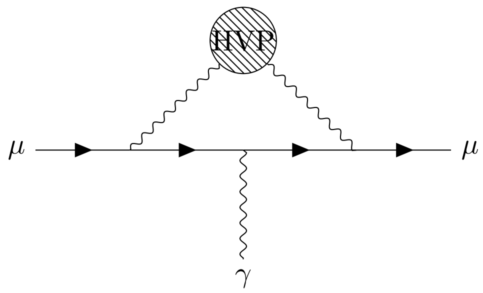

Hadronic vacuum-polarisation insertion; the blob represents non-perturbative QCD.

At low energy, quarks and gluons are strongly coupled, so ordinary perturbative QCD cannot determine the blob sufficiently accurately. Two complementary methods are used:

1. A data-driven dispersive calculation relates HVP to measured $e^+e^- \to$ hadrons cross sections using analyticity and unitarity. Low-energy data, especially the two-pion channel, carry the largest weight.
2. Lattice QCD computes Euclidean electromagnetic-current correlation functions from first principles and convolves them with a known kernel. Continuum, infinite-volume, physical-mass and isospin-breaking corrections must all be controlled.

HVP is the dominant uncertainty in the current Standard Model prediction and the source of the most important methodological tension.

5.10.4 Hadronic light-by-light scattering

In HLbL scattering, three internal photons connect the muon line to a hadronic four-current correlation function, while the external photon also couples to that hadronic subdiagram:

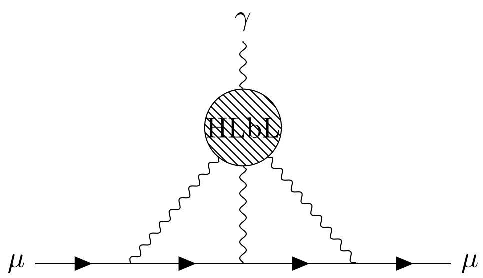

Hadronic light-by-light contribution; the blob denotes a hadronic four-current correlator.

HLbL cannot be reconstructed from one inclusive cross section. It is evaluated using dispersive methods, exclusive hadronic data and lattice-QCD four-point functions. Modern phenomenological and lattice determinations are mutually consistent within their uncertainties, and their average enters the 2025 recommendation.

5.10.5 Precision accounting

The 2025 Muon $g-2$ Theory Initiative gives the following contributions in units of 10^{-11} [8]:

Contribution	Recommended value	Precision highlight
QED	116 584 718.8(2)	known through $\mathcal{O}(\alpha^5)$
Electroweak	154.4(4)	complete two-loop calculation
HVP, leading order	7132(61)	lattice-QCD average
HVP, all quoted orders	7045(61)	dominates the total uncertainty
HLbL, including NLO	115.5(9.9)	phenomenology–lattice average
Total Standard Model	116 592 033(62)	HVP-limited

Here NLO means next-to-leading order. QED dominates the central value but is not the limiting uncertainty; the far smaller HVP contribution controls the precision.

5.10.6 Present comparison with experiment

The 2025 recommended Standard Model value is

$$\boxed{a_\mu^{\rm SM} = 116\,592\,033(62) \times 10^{-11}}. \tag{5.71}$$

Together with Eq. (5.69), this gives

$$\boxed{\Delta a_\mu \equiv a_\mu^{\rm exp} - a_\mu^{\rm SM} = 38(63) \times 10^{-11}.} \tag{5.72}$$

There is therefore no statistically significant tension between experiment and the 2025 recommended Standard Model value.

This differs from the widely reported comparison with the 2020 White Paper, which used a data-driven HVP recommendation and produced a discrepancy above five standard deviations when combined with later experimental results. The experimental central value did not move towards theory. Rather, the 2025 recommendation adopted a consolidated lattice-QCD HVP average that is larger and raises the Standard Model prediction towards experiment.

The problem is not fully closed. Lattice HVP calculations and several data-driven dispersive determinations do not yet make one completely consistent picture, and tensions also exist among some hadronic cross-section datasets. The measurement is now substantially more precise than the Standard Model prediction, so further progress is primarily limited by theory and hadronic input.

Key idea

Muon $g-2$ should no longer be described without qualification as an established five-standard-deviation failure of the Standard Model. The central question is whether independent lattice, dispersive and new experimental determinations of hadronic vacuum polarisation converge.

Connection to flavour. A heavy particle that contributes to the muon dipole usually also affects charged-lepton-flavour violation, electric dipole moments or collider processes. A proposed explanation of a_μ must therefore be tested as a correlated model rather than against one number alone.

5.11 Summary

The CKM matrix arises from Yukawa-matrix misalignment,

$$V_{\rm CKM} = U_{uL}^\dagger U_{dL}. \tag{5.73}$$

For three generations it contains three angles and one CP phase. Unitarity produces triangle relations, while the Jarlskog invariant gives a convention-independent measure of CP violation. Tree-level neutral currents remain flavour diagonal, and loop-level flavour change is further suppressed by the GIM mechanism.

Rare decays and neutral-meson mixing probe heavy virtual physics but require a controlled combination of short-distance Wilson coefficients and hadronic matrix elements. Current R_K and R_{K^*} results are compatible with the Standard Model; $R(D^{(*)})$ and inclusive–exclusive CKM determinations remain interesting tensions rather than discoveries.

The muon anomaly is the Pauli form factor $F_2(0)$. Its experimental value is known to about 124 ppb, but its interpretation is now limited by hadronic theory. The 2025 lattice-HVP-based Standard Model update agrees with experiment, while resolving HVP differences remains a central open problem.

Checkpoint

The precision-frontier logic is:

$$\begin{aligned}&\text{symmetry suppresses the Standard Model amplitude}\\ \Longrightarrow\quad &\text{small virtual contributions become visible.}\end{aligned}$$

The same logic underlies CKM tests, meson mixing, rare decays, CP violation and the anomalous magnetic moment.

Short exercises

1. Starting from the weak-basis charged current, derive $V_{\text{CKM}} = U_{uL}^{\dagger} U_{dL}$.
2. Draw the unitarity triangle from $V_{ud}V_{ub}^* + V_{cd}V_{cb}^* + V_{td}V_{tb}^* = 0$ and explain how tree- and loop-dominated measurements provide complementary tests.
3. Use CKM unitarity to show that the mass-independent part of Eq. (5.56) cancels.
4. Use dimensional analysis and chirality to motivate $\Delta a_\ell \propto m_\ell^2/\Lambda^2$.

Chapter 6

From the Standard Model to Grand Unification

Grand unification asks whether the three Standard Model gauge interactions are different low-energy manifestations of one interaction. Its economy is attractive, but experiment must decide whether it is realised.

The Standard Model gauge group is

$$G_{\mathrm{SM}} = SU(3)_C \times SU(2)_L \times U(1)_Y. \tag{6.1}$$

$SU(3)_C$ is the colour symmetry of the strong interaction, $SU(2)_L$ acts on left-handed weak doublets, and $U(1)_Y$ is weak hypercharge. The symbol $\times$ means that all three symmetries act, with independent couplings g_s, g and g'. A grand unified theory (GUT) embeds them in one larger group with one coupling at a high scale M_{GUT}:

$$G_{\mathrm{GUT}} \xrightarrow{M_{\mathrm{GUT}}} G_{\mathrm{SM}} \xrightarrow{v} SU(3)_C \times U(1)_{\mathrm{em}}. \tag{6.2}$$

The arrows denote spontaneous symmetry breaking, and $v \simeq 246\,\mathrm{GeV}$ is the electroweak vacuum expectation value. A GUT may explain charge quantisation and the organisation of matter, but it does not automatically explain three generations, Yukawa hierarchies, dark matter or gravity.

6.1 A minimal group-theory dictionary

A *representation* specifies how a field transforms under a symmetry. For $SU(N)$, the *fundamental representation* acts on an N-component column vector. A quark is therefore in the fundamental $\mathbf{3}$ of colour $SU(3)$, while a left-handed weak doublet is in the fundamental $\mathbf{2}$ of $SU(2)$. Bold numbers label representation dimensions, not numerical factors. A bar, as in $\overline{\mathbf{3}}$, denotes the complex-conjugate representation; a singlet $\mathbf{1}$ is unchanged by that group.

The generators T^a describe infinitesimal transformations, $\psi \to (1 + i\theta^a T^a)\psi$, where θ^a are small real parameters and the repeated index a is summed. $SU(N)$ has $N^2 - 1$ generators. Its gauge bosons carry the generator label and transform among themselves in the *adjoint representation*, also of dimension $N^2 - 1$. Thus the eight gluons form the adjoint $\mathbf{8}$ of $SU(3)$ and the three weak bosons form the adjoint $\mathbf{3}$ of $SU(2)$.

We use

$$(\mathbf{d}_3, \mathbf{d}_2)_Y \tag{6.3}$$

for an $SU(3)_C$ representation of dimension r_3, an $SU(2)_L$ representation of dimension r_2, and hypercharge Y. Electric charge is $Q = T_3 + Y$. For example, $(\mathbf{3}, \mathbf{2})_{1/6}$ is a colour triplet and weak doublet; its components with $T_3 = +1/2$ and $-1/2$ have charges $+2/3$ and $-1/3$.

6.2 Running couplings: why unification can be hidden

A quantum-field-theory coupling depends on the energy at which it is measured. Virtual particles screen or anti-screen a charge, and a higher-energy probe resolves a different range of quantum fluctuations. This energy dependence is called *running*; it is not variation with time.

For gauge factor $i = 1, 2, 3$, the one-loop renormalisation-group equation is

$$\mu \frac{\mathrm{d}g_i}{\mathrm{d}\mu} = \frac{b_i}{16\pi^2} g_i^3, \qquad \boxed{\alpha_i^{-1}(\mu) = \alpha_i^{-1}(\mu_0) - \frac{b_i}{2\pi} \ln \frac{\mu}{\mu_0}}, \tag{6.4}$$

where μ is the probe energy, μ_0 is a reference energy, $g_i(\mu)$ is the coupling, and $\alpha_i \equiv g_i^2/(4\pi)$. The constants b_i are beta-function coefficients fixed by the gauge and matter fields. Consequently, plotting α_i^{-1} against $\ln \mu$ gives approximately straight lines, with different b_i producing different slopes.

For a GUT comparison one conventionally writes

$$g_1 = \sqrt{\frac{5}{3}}\, g', \qquad g_2 = g, \qquad g_3 = g_s, \tag{6.5}$$

using the hypercharge normalisation inherited from $SU(5)$. The factor $5/3$ is not a new interaction. With Standard Model particles,

$$(b_1, b_2, b_3)_{\mathrm{SM}} = \left(\frac{41}{10}, -\frac{19}{6}, -7\right), \tag{6.6}$$

and the three inverse couplings approach but do not meet exactly. With the minimal supersymmetric Standard Model (MSSM) spectrum,

$$(b_1, b_2, b_3)_{\mathrm{MSSM}} = \left(\frac{33}{5}, 1, -3\right), \tag{6.7}$$

their convergence near 10^{16} GeV improves. This is suggestive, not proof. Crossing a particle mass threshold activates new quantum fluctuations, changes b_i, and hence changes a line's slope. Two-loop effects and unknown high-scale thresholds also affect the apparent meeting point.

Key idea

A unification plot is conditional on the assumed particle spectrum. Approximately intersecting lines motivate unification but do not establish a particular theory.

6.3 $SU(5)$: the minimal worked example

$SU(5)$ consists of unitary 5×5 matrices with determinant one. It has $5^2 - 1 = 24$ generators, so its 24 gauge bosons form the adjoint $\mathbf{24}$. The first three components may be associated with colour and the final two with weak isospin. Hypercharge is embedded as the traceless matrix

$$Y = \mathrm{diag}\left(-\frac{1}{3}, -\frac{1}{3}, -\frac{1}{3}, \frac{1}{2}, \frac{1}{2}\right), \tag{6.8}$$

where diag denotes a diagonal matrix. Its entries sum to zero, as required for an $SU(5)$ generator. This embedding fixes relative hypercharges and explains charge quantisation.

Under the Standard Model subgroup, the adjoint splits as

$$\begin{aligned} \mathbf{24} = {} & (\mathbf{8}, \mathbf{1})_0 \oplus (\mathbf{1}, \mathbf{3})_0 \oplus (\mathbf{1}, \mathbf{1})_0 \\ & \oplus (\mathbf{3}, \mathbf{2})_{-5/6} \oplus (\overline{\mathbf{3}}, \mathbf{2})_{5/6}. \end{aligned} \tag{6.9}$$

$\oplus$ means that one representation separates into the listed independent parts. The first three contain the gluons, weak bosons and hypercharge boson. The final two contain twelve heavy X, Y gauge bosons carrying colour and weak quantum numbers, which can convert quarks into leptons.

An adjoint scalar Σ can acquire

$$\langle\Sigma\rangle \propto \mathrm{diag}(2, 2, 2, -3, -3). \tag{6.10}$$

Angle brackets mean vacuum expectation value and $\propto$ means "proportional to." This leaves the Standard Model gauge bosons massless at the GUT scale but gives X, Y masses $M_X \sim g_5 M_{\mathrm{GUT}}$, where g_5 is the unified coupling.

A Weyl field describes a fermion with a definite chirality. A *left-handed Weyl field* satisfies

$$P_L\psi = \psi, \qquad P_L = \frac{1-\gamma^5}{2}, \tag{6.11}$$

where P_L is the left-handed chiral projector and γ^5 is the chirality matrix. Similarly, $P_R = (1+\gamma^5)/2$ selects a right-handed field. A four-component Dirac fermion can be constructed from one left-handed and one right-handed Weyl field.

For group-theory bookkeeping, it is convenient to express every fermion as a left-handed Weyl field. A physical right-handed field f_R is therefore replaced by its left-handed charge-conjugate field,

$$f_L^c \equiv C\,\overline{f_R}^{\,T}, \tag{6.12}$$

where C is the charge-conjugation matrix and T denotes transpose. The field f_L^c has the opposite gauge quantum numbers to f_R. For example, the right-handed up quark transforms as a colour $\mathbf{3}$ with electric charge $+2/3$, whereas its left-handed charge-conjugate u^c transforms as an $\overline{\mathbf{3}}$ with charge $-2/3$. These are two descriptions of the same physical degrees of freedom, not an additional antiparticle.

With this convention, all fermions of one Standard Model generation can be listed as left-handed fields:

$$Q = (u_L, d_L)^T, \qquad L = (\nu_L, e_L)^T, \qquad u^c, \quad d^c, \quad e^c. \tag{6.13}$$

They can then be arranged naturally into the two $SU(5)$ representations $\overline{\mathbf{5}}$ and $\mathbf{10}$.

Using this all-left-handed Weyl-field convention, one Standard Model generation fits into

$$\overline{\mathbf{5}} = (\overline{\mathbf{3}}, \mathbf{1})_{1/3} \oplus (\mathbf{1}, \mathbf{2})_{-1/2} \supset (d^c, L), \tag{6.14}$$

$$\mathbf{10} = (\mathbf{3}, \mathbf{2})_{1/6} \oplus (\overline{\mathbf{3}}, \mathbf{1})_{-2/3} \oplus (\mathbf{1}, \mathbf{1})_1 \supset (Q, u^c, e^c). \tag{6.15}$$

Here $Q = (u_L, d_L)^T$ and $L = (\nu_L, e_L)^T$ are weak doublets; T means transpose. The superscript c denotes the left-handed charge-conjugate field corresponding to a right-handed fermion, and $\supset$ means "contains." The 15 Standard Model Weyl fields have become a $\overline{\mathbf{5}}$ and a $\mathbf{10}$, whose gauge anomalies cancel.

The Higgs can lie in

$$\mathbf{5}_H = (\mathbf{3}, \mathbf{1})_{-1/3} \oplus (\mathbf{1}, \mathbf{2})_{1/2}. \tag{6.16}$$

Together with the familiar weak doublet, this contains a coloured scalar that must be extremely heavy. Explaining this enormous mass difference is the *doublet–triplet splitting problem.* Minimal $SU(5)$ also predicts $Y_d = Y_e^T$ at the GUT scale, relating down-quark and charged-lepton Yukawa matrices; this fails for the lighter generations without extra structure.

6.4 Proton decay: the decisive consequence

In $SU(5)$, X, Y exchange connects quarks and leptons. At energies well below the heavy mass, its propagator becomes approximately $1/M_X^2$, producing

$$\mathcal{L}_{\text{eff}} \sim \frac{g_5^2}{M_X^2}(qq)(q\ell) + \text{h.c.}, \tag{6.17}$$

where q and ℓ denote quark and lepton fields and h.c. means Hermitian conjugate. This permits $p \to e^+\pi^0$. Dimensional analysis gives

$$\Gamma_p \sim \alpha_G^2 \frac{m_p^5}{M_X^4} \times (\text{flavour, running and hadronic factors}), \qquad \tau_p = \Gamma_p^{-1} \propto M_X^4, \tag{6.18}$$

where Γ_p, τ_p and m_p are the proton decay rate, lifetime and mass, and $\alpha_G = g_5^2/(4\pi)$. Precise predictions need operator running and lattice-QCD matrix elements. Minimal non-supersymmetric $SU(5)$ has inadequate coupling unification and proton decay that is too rapid, so that minimal model is excluded; grand unification in general is not.

Experimental connection

For $p \to e^+\pi^0$, a water Cherenkov detector searches for an electron-like ring and two photons from $\pi^0 \to \gamma\gamma$. Super-Kamiokande finds

$$\tau/B(p \to e^+\pi^0) > 2.4 \times 10^{34}\ \text{yr}$$

at 90% confidence [9], where B is the branching fraction. Hyper-Kamiokande will provide much greater exposure [10]; liquid-argon detectors complement it for kaon modes.

6.5 $SO(10)$, neutrino mass and the seesaw

$SO(10)$ is a larger unified group. Its spinor representation **16** contains a full generation, including a right-handed neutrino:

$$\mathbf{16} = \mathbf{10} \oplus \overline{\mathbf{5}} \oplus \mathbf{1} \qquad \text{under } SU(5). \tag{6.19}$$

"Spinor" merely names this representation; its construction is not required here. The singlet **1** corresponds to ν_R, and $SO(10)$ also contains $B - L$, baryon number minus lepton number.

Because ν_R is a Standard Model singlet, it may have a large Majorana mass M_R. In the basis (ν_L, ν_R^c),

$$\mathcal{M}_\nu = \begin{pmatrix} 0 & m_D \\ m_D^T & M_R \end{pmatrix}, \qquad \boxed{m_\nu \simeq -m_D M_R^{-1} m_D^T} \quad (M_R \gg m_D). \tag{6.20}$$

m_D is the Dirac mass matrix, T denotes transpose, and M_R^{-1} denotes the matrix inverse. The inverse heavy scale naturally makes m_ν small.

Below M_R, the same physics is described by the Weinberg operator,

$$\mathcal{L}_5 = \frac{c_{ij}}{\Lambda}(\overline{L_i^c}\widetilde{\Phi}^*)(\widetilde{\Phi}^\dagger L_j) + \text{h.c.}, \qquad m_\nu \sim \frac{cv^2}{\Lambda}. \tag{6.21}$$

i, j label generations, c_{ij} are dimensionless coefficients, Λ is the heavy scale, Φ is the Higgs doublet, and $\widetilde{\Phi} = i\sigma_2\Phi^*$ is its conjugate. This dimension-five operator violates lepton number by two units and gives Majorana masses after electroweak symmetry breaking. Neutrinoless double-beta decay can test this; heavy-neutrino decays may also support leptogenesis, although that is model dependent.

6.6 What can low-energy experiments really test?

Heavy GUT particles leave low-energy effective interactions,

$$\mathcal{L}_{\text{eff}} = \mathcal{L}_{\text{SM}} + \frac{c_5}{\Lambda}\mathcal{O}_5 + \frac{c_6}{\Lambda^2}\mathcal{O}_6 + \cdots . \tag{6.22}$$

$\mathcal{O}_d$ is an operator of mass dimension d, while c_d is a dimensionless coefficient. Dimension-five operators can generate Majorana neutrino masses; dimension-six operators can produce proton decay or rare flavour processes. Different measurements probe different coefficients, flavour rotations and masses, so there is no model-independent experimentally measured GUT scale.

Key idea

A GUT becomes predictive only after its symmetry-breaking chain, heavy spectrum and flavour structure are specified. Coupling running, proton decay, neutrino masses and flavour limits must then be tested together.

6.7 Summary

A fundamental representation acts on a basic multiplet of fields; the adjoint describes gauge bosons associated with the generators. $SU(5)$ explains charge quantisation and embeds one generation in $\overline{\mathbf{5}} \oplus \mathbf{10}$, while predicting baryon-violating X, Y bosons. $SO(10)$ also contains ν_R and accommodates the seesaw. Running couplings motivate unification, but their evolution depends on the particle spectrum. Proton decay, neutrino properties, flavour observables and new-particle searches provide the experimental tests.

Checkpoint

The route through the course is

$$\text{Fermi theory} \to SU(2)_L \times U(1)_Y \to \text{Higgs mechanism}$$
$$\to \text{precision and flavour tests} \to \text{possible GUT structure.}$$

Symmetry reduces arbitrariness; experiment decides whether it is realised.

Short exercises

1. Integrate the one-loop beta function to derive Eq. (6.4). Why does a new threshold change the slope?
2. Verify that Eq. (6.8) is traceless. Use $Q = T_3 + Y$ to check the charges of $(\mathbf{3}, \mathbf{2})_{1/6}$.
3. Explain why integrating out X gives g_5^2/M_X^2 and why $\tau_p \propto M_X^4$.
4. Estimate M_R from $m_\nu \simeq y^2v^2/(2M_R)$ for $m_\nu = 0.05\,\text{eV}$ and Yukawa coupling $y = 1$.

Bibliography

[1] J. Iliopoulos, "Introduction to the Standard Model of the Electro-Weak Interactions," in *Proceedings of the 2015 CERN–Latin-American School of High-Energy Physics*, CERN-2016-005.

[2] A. Pich, "The Standard Model of Electroweak Interactions," lecture notes in CERN Yellow Reports.

[3] C. Quigg, "The Electroweak Theory," arXiv:hep-ph/0204104.

[4] A. B. Arbuzov, "Quantum Field Theory and the Electroweak Standard Model," arXiv:1801.05670.

[5] LHCb Collaboration, "Test of lepton universality in $b \to s\ell^+\ell^-$ decays," *Phys. Rev. Lett.* **131** (2023) 051803, arXiv:2212.09152.

[6] Heavy Flavor Averaging Group, "HFLAV results and world averages," `https://hflav.web.cern.ch/results`, accessed September 2026.

[7] Muon $g-2$ Collaboration, "Measurement of the Positive Muon Anomalous Magnetic Moment to 127 ppb," arXiv:2506.03069.

[8] Muon $g-2$ Theory Initiative, "The anomalous magnetic moment of the muon in the Standard Model: an update," *Phys. Rept.* **1143** (2025) 1, arXiv:2505.21476.

[9] Super-Kamiokande Collaboration, "Search for proton decay via $p \to e^+\pi^0$ and $p \to \mu^+\pi^0$," *Phys. Rev. D* **102** (2020) 112011, arXiv:2010.16098.

[10] Hyper-Kamiokande Proto-Collaboration, "Hyper-Kamiokande Design Report," arXiv:1805.04163.

[11] Particle Data Group, "Review of Particle Physics," *Prog. Theor. Exp. Phys.* (2024) 083C01.

[12] D. Gross and F. Wilczek, "Ultraviolet Behavior of Non-Abelian Gauge Theories," *Phys. Rev. Lett.* **30** (1973) 1343.

[13] H. D. Politzer, "Reliable Perturbative Results for Strong Interactions?," *Phys. Rev. Lett.* **30** (1973) 1346.

[14] C. S. Wu *et al.*, "Experimental Test of Parity Conservation in Beta Decay," *Phys. Rev.* **105** (1957) 1413.

[15] F. J. Hasert *et al.* (Gargamelle Collaboration), "Observation of Neutrino-like Interactions Without Muon or Electron in the Gargamelle Neutrino Experiment," *Phys. Lett. B* **46** (1973) 138.

[16] UA1 Collaboration, "Experimental Observation of Isolated Large Transverse Energy Electrons with Associated Missing Energy at $\sqrt{s} = 540$ GeV," *Phys. Lett. B* **122** (1983) 103.

[17] UA2 Collaboration, "Observation of Single Isolated Electrons of High Transverse Momentum in Events with Missing Transverse Energy at the CERN Proton–Antiproton Collider," *Phys. Lett. B* **122** (1983) 476.

[18] J. Schwinger, "On Quantum-Electrodynamics and the Magnetic Moment of the Electron," *Phys. Rev.* **73** (1948) 416.

[19] J. H. Christenson, J. W. Cronin, V. L. Fitch and R. Turlay, "Evidence for the 2π Decay of the K_2^0 Meson," *Phys. Rev. Lett.* **13** (1964) 138.

[20] Y. Fukuda *et al.* (Super-Kamiokande Collaboration), "Evidence for Oscillation of Atmospheric Neutrinos," *Phys. Rev. Lett.* **81** (1998) 1562.

[21] Q. R. Ahmad *et al.* (SNO Collaboration), "Measurement of the Rate of $\nu_e + d \to p + p + e^-$ Interactions Produced by ^{8}B Solar Neutrinos," *Phys. Rev. Lett.* **87** (2001) 071301.

[22] TASSO Collaboration, "Evidence for Planar Events in e^+e^- Annihilation at High Energies," *Phys. Lett. B* **86** (1979) 243.

[23] M. E. Peskin and D. V. Schroeder, *An Introduction to Quantum Field Theory*, Westview Press (1995).

[24] F. Halzen and A. D. Martin, *Quarks and Leptons: An Introductory Course in Modern Particle Physics*, Wiley (1984).

[25] M. Thomson, *Modern Particle Physics*, Cambridge University Press (2013).

[26] S. Weinberg, *The Quantum Theory of Fields, Vol. II: Modern Applications*, Cambridge University Press (1996).

[27] C. Quigg, *Gauge Theories of the Strong, Weak, and Electromagnetic Interactions*, Princeton University Press (2013).

[28] P. Langacker, *The Standard Model and Beyond*, CRC Press (2010).

[29] I. Aitchison and A. Hey, *Gauge Theories in Particle Physics*, CRC Press (2012).

[30] D. Griffiths, *Introduction to Elementary Particles*, Wiley-VCH (2008).

[31] G. Altarelli, "The Standard Model of Particle Physics," *La Rivista del Nuovo Cimento* **37** (2014) 321–403.

[32] A. Djouadi, "The Anatomy of Electro-Weak Symmetry Breaking. I: The Higgs Boson in the Standard Model," *Phys. Rept.* **457** (2008) 1–216.